



저작자표시-비영리-변경금지 2.0 대한민국

이용자는 아래의 조건을 따르는 경우에 한하여 자유롭게

- 이 저작물을 복제, 배포, 전송, 전시, 공연 및 방송할 수 있습니다.

다음과 같은 조건을 따라야 합니다:



저작자표시. 귀하는 원저작자를 표시하여야 합니다.



비영리. 귀하는 이 저작물을 영리 목적으로 이용할 수 없습니다.



변경금지. 귀하는 이 저작물을 개작, 변형 또는 가공할 수 없습니다.

- 귀하는, 이 저작물의 재이용이나 배포의 경우, 이 저작물에 적용된 이용허락조건을 명확하게 나타내어야 합니다.
- 저작권자로부터 별도의 허가를 받으면 이러한 조건들은 적용되지 않습니다.

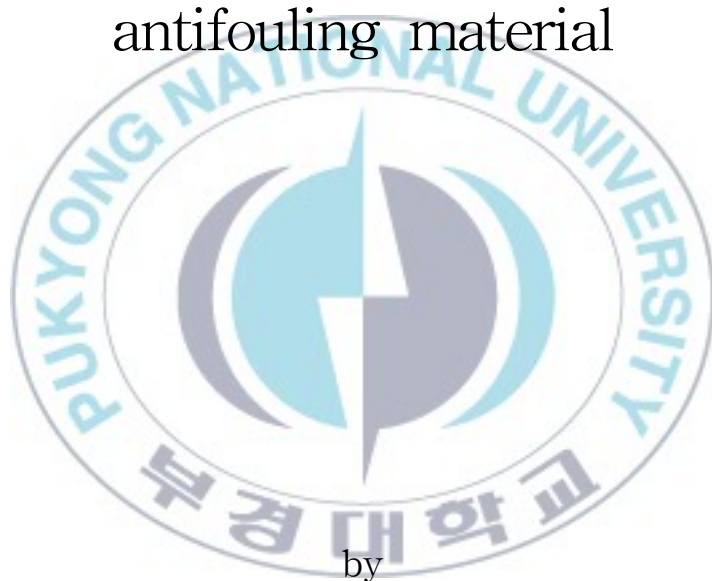
저작권법에 따른 이용자의 권리는 위의 내용에 의하여 영향을 받지 않습니다.

이것은 [이용허락규약\(Legal Code\)](#)을 이해하기 쉽게 요약한 것입니다.

[Disclaimer](#)

Thesis for the Degree of Doctor of Engineering

Biological analysis on coralline algae
and periostracum of blue mussel for
antifouling material



by

Ji-Young Kang

Department of Biotechnology

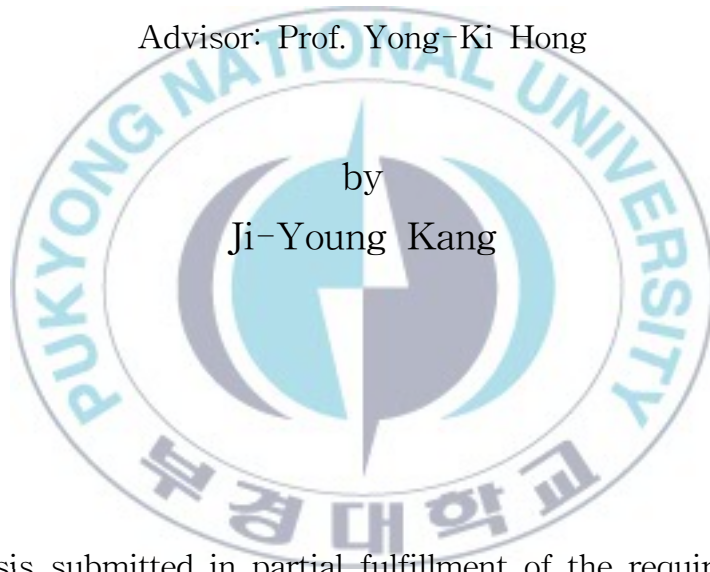
The Graduate School

Pukyong National University

August 2013

Biological analysis on coralline algae and periostracum
of blue mussel for antifouling material
(방오소재 개발을 위한 산호조류 및
진주담치 각피의 생물학적 특성)

Advisor: Prof. Yong-Ki Hong



by
Ji-Young Kang

A thesis submitted in partial fulfillment of the requirements
for the degree of

Doctor of Engineering

in Department of Biotechnology, The Graduate School,
Pukyong National University

August 2013

Biological analysis on coralline algae and periostracum
of blue mussel for antifouling material

A dissertation

by

Ji-Young Kang

Approved by:

Nam Gyu Park, Ph. D.
(Chairman)

Dong Soo Hwang, Ph. D.
(Member)

Il Soo Moon, Ph. D.
(Member)

Joong Kyun Kim, Ph. D.
(Member)

Yong Ki Hong, Ph. D.
(Member)

August 23, 2013

CONTENT

List of Table	iii
List of Figure	iv
Abstract	vi

Chapter I

General Introduction	1
----------------------	---

Chapter II

Biological characteristics and tissue structure of a crustose coralline *Lithophyllum* Alga

Abstract	9
Introduction	10
Materials and Methods	11
Results	14
Discussion	17
References	26

Chapter III

Biological characteristics and tissue structure of the branched coralline Alga *Corallina pilulifera*

Abstract	30
Introduction	31
Materials and Methods	32
Results	36
Discussion	38
References	47

Chapter IV

Effect of calcification inhibitors on the viability of the coralline algae

Abstract	52
Introduction	53
Materials and Methods	56
Results	58
Discussion	59
References	65

Chapter V

Antifouling activity of extracts of the periostracum of the mussel *Mytilus edulis*

Abstract	68
Introduction	69
Materials and Methods	71
Results	74
Discussion	76
References	83

Summary in Korea	85
------------------------	----

Acknowledgements	87
------------------------	----

List of Tables

Table 2-1.	Profile of the major fatty acids (% of total fatty acids) in the crustose coralline tissue collected on February 9, 2012.	25
Table 3-1.	Profile of the major fatty acids (% of total fatty acids) in <i>Corallina pilulifera</i> tissue collected on December 22, 2012.	46
Table 4-1.	Effect of calcification inhibitors on viability of the coralline <i>Lithophyllum yessoense</i>	61
Table 4-2.	Effect of calcification inhibitors on viability of the coralline <i>Corallina pilulifera</i>	62
Table 5-1.	Effects of extracts from fresh and acidified periostracum on settlement of <i>Porphyra suborbiculata</i> monospores.	80
Table 5-2.	Effects of extracts from fresh and acidified periostracum on germination of <i>Porphyra suborbiculata</i> monospores.	81
Table 5-3.	Compounds identified from dichloromethane extracts of periostracum by GC-MS.	82

List of Figures

Figure 2-1.	18S rDNA sequence (1391 base) of the crustose coralline alga.	20
Figure 2-2.	Phylogenetic dendrograms of the crustose coralline alga based on 18S rDNA sequence, and constructed using the neighbor-joining method.	21
Figure 2-3.	Seasonal variation in the viability of the crustose coralline tissue.	22
Figure 2-4.	Effect of various parameters on the optimal maintenance of the crustose coralline tissue.	23
Figure 2-5.	Tissue of the articulated coralline alga.	24
Figure 3-1.	Tissue of the articulated coralline alga (A) and medullary tiers in longitudinal sections through the axial intergeniculum (B).	41
Figure 3-2.	Phylogenetic dendrograms of the coralline alga (CP) based on 18S rDNA (A), psbA (B), and rbcL (C) sequences, and constructed using the neighbor-joining method.	42
Figure 3-3.	Seasonal variation in the viability of <i>Corallina pilulifera</i> tissue.	43
Figure 3-4.	Effect of various parameters on the optimal maintenance of <i>Corallina pilulifera</i> tissue	44
Figure 3-5.	Scanning electron micrograph of <i>Corallina pilulifera</i> tissue	45

Figure 4-1.	Effect of Fe-citrate on <i>Lithophyllum yessoense</i> tissue.	63
Figure 4-2.	Effect of Fe-citrate on <i>Corallina pilulifera</i> tissue.	64
Figure 5-1.	Periostracum of blue mussel <i>Mytilus edulis</i> .	78
Figure 5-2.	Settlement of <i>Porphyra suborbiculata</i> monospores on periostracum of <i>M. edulis</i> .	79



Biological characteristics and algicidal substance against the biofouling
coralline algae

Ji-Young Kang

Department of Biotechnology, The Graduate School,
Pukyong National University

Abstract

We plan to search antifouling materials from the coralline algae to prevent biofouling damage to ship or marine structure. Bio-mimic materials would become an environmental-friendly and no harmful source to the marine application. The coralline algae shows one of main reasons of algal whitening in barren ground where has no seaweed growth, and also shows allelopathic effect against attachment and germination of seaweed spores. Bio-mimic materials of the coralline algae might be usable as antifouling agents against seaweed at least. Gene analysis, viability assay, treatment of calcification inhibitors, and related researches will be done in this study.

The disappearance of seaweed flora in some rocky areas, known as algal whitening, barren ground, coralline flats, or deforested areas, is associated with some species of coralline algae. To determine the biological characteristics of a representative species of crustose coralline alga, 18S rDNA gene was sequenced to identify the genus *Lithophyllum*. By morphological and distributional characteristics, it is deduced to *L. yessoense*. Measuring viability using triphenyl tetrazolium chloride showed highly viability from December to February. Cultural conditions of 16 °C, a 16 hr light:8 hr dark cycle, and 30 $\mu\text{E m}^{-2}\text{s}^{-1}$ light intensity were optimal for maintaining the viability of the alga for up to 5 days. The fatty acids included 9.7% ω -3 eicosapentaenoic acid. Scanning electron microscopy of the surface structure revealed round craters about 3.6 μm in diameter, covered with rough irregular and angular polygon-shaped structures about 1.0 to 3.7 μm in size. Biomimetic coralline alga based on the composition and structure

might become an environmentally friendly antifouling material against the attachment of soft foulants.

The decrease in the seaweed flora in some rocky areas, known as algal whitening or barren ground, is associated with some species of coralline algae. To determine the biological characteristics of a representative species of branched coralline alga, the number of medullary tiers was counted and ranged from 12 to 16. The 18S rDNA, *psbA*, and *rbcL* genes were used to confirm the identification of *Corallina pilulifera*. Measuring viability using triphenyl tetrazolium chloride showed highly viability from December to January. Cultural conditions of 16 °C, a 16 h light:8 h dark cycle, and 40 $\mu\text{E m}^{-2}\text{s}^{-1}$ light intensity were optimal for maintaining the viability of the coralline alga for up to 3 days. The fatty acids included 31.4% ω -3 eicosapentaenoic acid. Scanning electron microscopy of the surface structure revealed unique round wells about $7.9 \pm 1.3 \mu\text{m}$ in diameter.

The addition of calcification inhibitors was found to regulate the viability of cultures of the coralline alga *Lithophyllum yessoense* and *Corallina pilulifera*. The viability was quantitated using a triphenyltetrazolium chloride assay, and the eight of different calcification inhibitors were tested. Fe-citrate and FeCl_2 inhibited viability, and dichloromethylenediphosphonic acid increased viability. The Fe-citrate, which had the strongest inhibitory activity, decreased viability to 74 and 12% that of the control following addition of 1 mM or 10 mM of culture media of *L. yessoense*, respectively. Even *C. pilulifera* culture media, Fe-citrate inhibited viability to 63 and 44% that of the control following addition of 1 mM or 10 mM. The Fe-citrate suppressed *L. yessoense* and *C. pilulifera* viability the most.

A study was made to investigate possible formation by the periostracum of the mussel *Mytilus edulis* of antifouling substances against the settlement and germination of spores of *Porphyra suborbiculata*. The shell coating known as the periostracum, is indicated as a possible physical and chemical antifouling defense component. The periostracum was separated from the shell and extracts of the periostracum obtained by extraction with three solvents. Considerable activity against monospores was shown by ethyl acetate and dichloromethane extract. The microtopography of the shell surface was measured using scanning electron microscopy (SEM) which revealed homogeneous and ridged surface of periostracum. The periostracum surface

has also shown considerable activity against monospores. This indicates that in mussels *P. suborbiculata* the periostracum possesses a generic anti-settlement property, at least against spores settlement and germination.



Chapter I

General Introduction



Fouling is the accumulation of unwanted material on solid surfaces to the detriment of function. The fouling material can consist of either living organisms (biofouling) or a non-living substance (inorganic or organic). Fouling is usually distinguished from other surface-growth phenomena in that it occurs on a surface of a component, system or plant performing a defined and useful function, and that the fouling process impedes or interferes with this function.

Barnacles

Barnacles are the most commonly encountered fouling animal. Barnacle larvae are selective in their site for settlement and appear to recognise other barnacles. This results in barnacles settling close to other members of the species which aids in cross fertilisation. Barnacles live within hard calcareous shells which can adhere very tightly and can be difficult to remove. On ships, removal by underwater scrubbing or mechanical scraping typically results in a barnacle residue being left behind. This can promote further colonisation, increasing the fouling problem. Gooseneck barnacles These animals are especially adapted for life attached to moving objects. Gooseneck barnacles are unusual in that they are not a coastal or shoreline fouling problem but can settle on moving ships' hulls in the open ocean.

Hydroids

Plant like in appearance, hydroids live in colonies and are often found on the flat bottom of vessels where they are often mistaken for algae. Due to the low light levels on flat bottom areas, however, it is

a safe assumption that filamental growth on the flat bottom is likely to be a type of hydroid and not algae.

Molluscs

These are animals with hard, paired shells such as mussels and oysters. Adhesion to submerged structures is relatively weak and this tends to limit settlement to stationary structures rather than on active vessels e.g. oil platforms.

Tube worms

These organisms live in easily recognisable calcareous tubes which protect their soft bodies. Tube worm larvae can recognise their own species resulting in large colonies being established. They tend to settle on stationary structures or on vessels which spend a comparatively longer time in port. Animal fouling does not require light to grow and can proliferate on any area of an underwater hull, including the flat bottom.

Seaweed

The most common plant fouling on ships is the brown algae *Ectocarpus spp.* and the green algae *Enteromorpha spp.*, often referred to as sea grass due to its similar appearance and colour. Polycellular algae begins with the settlement of microscopic spores. These spores can settle in seconds and colonise a submerged surface within hours. Plant fouling usually occurs where there is available sunlight, i.e. around the water line and a few metres below. It is not usually found on the flat bottom of vessels.

Slime

Slime on submerged surfaces is attributable to the accumulation of diatoms. Difficult to control, slime has a very low surface profile and can remain adherent on ships' hulls at speeds in excess of 30 knots. Slime fouling Slime on submerged surfaces is attributable to the accumulation of diatoms. Difficult to control, slime has a very low surface profile and can remain adherent on ships' hulls at speeds in excess of 30 knots.

Fouling organisms cause considerable damage to the immersed surfaces of man-made structures such as ships, fishnets, and aquaculture facilities. It can seriously impair the operational efficiency of a ship. Fuel represents around 50% of the operating costs of the Marine Transport Industry. Annual consumption of bunker fuel of the world's fleet is estimated at 180 million tonnes, which at current prices (approx. \$150/ tonne) is worth \$23 billion. A very rough fouled hull can increase fuel usage by as much as 40%, although typically a 100% weed fouled hull would result in a fuel penalty of 10%. If the world's fleet didn't have effective antifouling protection an estimated extra 72 million tonnes of fuel would be burned each year. This increased fuel consumption would lead to the production and release into the environment of an estimated extra 210 million tonnes of carbon dioxide (greenhouse gas) and 5.6 million tonnes of sulphur dioxide (acid rain).

Most antifouling techniques rely in a coating containing such

antifoulants as Irgarol, chlorothalonil, and diuron (Voulvoulis et al. 2000). However these antifoulants are toxic (Yamada 2007), and many studies have reported detecting these antifoulants in water and sediments samples in various aquatic environments (Voulvoulis 2006; Dafforn et al. 2011; Matthai et al. 2009). To develop environmentally sustainable antifouling agents, recent research has been focused on the behavior of microorganisms, biofilm formation and metabolite production which can inhibit marine invertebrate larval settlement and the attachment of algal spores (Cho et al. 2012).

Biomimetics is defined as the study of the structure and function of biological systems and processes as models or inspiration for the sustainable design and engineering of materials and machines (Salta et al. 2010). One of the interesting developments in the area of green tribology over the past 10 years is the recognition that nature has developed many highly optimized tribological surfaces that are: (i) typically multifunctional, (ii) reactive to their environment, and (iii) use a combination of physical and biological design strategies. The thalli of many marine algae and the surfaces of invertebrates are covered in mucilage or slime, which could render the attachment of fouling spores difficult or effect the removal of epibionts by continuous or periodic surface renewal (Wahl 1989). The role of surface sloughing in the removal of bacterial fouling in *Chondrus crispus* has been observed (Sieburth and Tootle 1981), and the colonial ascidian *Polysyncraton lacazei* has been found to shed a thin surface cuticle with its attached

epibionts at irregular intervals (Wahl & Banaigs 1991). The strategies evolved by marine organisms to resist epibiosis rely on four main mechanisms that can be broadly classified as employing chemical, physical, mechanical or behavioural effects (Ralston and Swain 2009).

This exciting new branch of antifouling research is truly multi-disciplinary, drawing from expertise in microbiology, engineering and materials science, in order to establish modern biomimetic antifouling technologies. The design of novel antifouling coatings has broadened to encompass natural products research, surface chemistry modulation and biomimetic surface development (Salta et al. 2010). However, as others have remarked, it is probable that any future broad-spectrum fouling-resistant surface will draw on several, if not all, of these diverse research areas to facilitate its efficacy. Ideally, an effective biomimetic antifouling coating will have the following properties: at least 5 years biofouling life-cycle control, durable and resistant to damage, repairable, low maintenance, easy to apply, hydraulically smooth, compatible with existing anticorrosion coatings, cost effective, non-toxic to non-target species and effective in port and at sea (Ralson & Swain 2009).

Reference

- Cho JY, Kang JY, Hong YK, Baek HH, Shin HW, Kim MS. 2012. Isolation and Structural Determination of the Antifouling Diketopiperazines from Marine-Derived *Streptomyces praecox* 293-11. *Bioscience Biotechnology and Biochemistry* 76: 1116-1121.
- Dafforn KA, Lewis JA, Johnston EL. 2011. Antifouling strategies: History and regulation, ecological impacts and mitigation. *Marine Pollution Bulletin* 62: 453-465.
- Dobretsova S, Teplitskib M, Paul V. 2009. Mini-review: quorum sensing in the marine environment and its relationship to biofouling. *Biofouling* 25: 413 - 427.
- Matthai C, Guise K, Coad P, McCready S, Taylor S. 2009. Environmental status of sediments in the lower Hawkesbury-Nepean River, New South Wales. *Australian Journal of Earth Sciences* 56: 225-243.
- Ralston E, Swain G. 2009 Bioinspiration—the solution for biofouling control? *Bioinspiration & Biomimetics* 4: 015007.
- Salta M, Wharton JA, Stoodley P, Dennington SP, Goodes LR, Werwinski S, Mart U, Wood RJK, Stokes KR. 2010. Designing biomimetic antifouling surfaces. *Philosophical Transactions of the Royal Society* 368: 4729-4754.
- Sieburth, J. M. & Tootle, J. L. 1981 Seasonality of microbial fouling on

Ascophyllum nodosum (L.) Lejol., *Fucus vesiculosus* L.,
Polysiphonia lanosa (L.) Tandy and *Chondrus crispus* Stackh.
Journal of Phycology 17 57 - 64.

Voulvoulis N, Scrimshaw MD, Lester JN. 2000. Occurrence of Four Biocides Utilized in Antifouling Paints, as Alternatives to Organotin Compounds, in Waters and Sediments of a Commercial Estuary in the UK. Marine Pollution Bulletin 40: 938 - 946.

Voulvoulis N. 2006. Antifouling paint booster biocides: occurrence and partitioning in water and sediments. The Handbook of Environmental Chemistry 50: 155-170.

Wahl M. 1989 Marine epibiosis. I. Fouling and antifouling: some basic aspects. Marine Ecology Progress Series 58: 175 - 189.

Wahl, M. & Banaigs, B. 1991 Marine epibiosis. III. Possible antifouling defense adaptations in *Polysyncraton lacazei* (Giard) (Didemnidae, Ascidiacea). Journal of Experimental Marine Biology and Ecology 145: 49 - 63.

Yamada H. 2007. Behaviour, occurrence, and aquatic toxicity of new antifouling biocides and preliminary assessment of risk to aquatic ecosystems. Bulletin of Fisheries Research Agency 21: 31-45.

Chapter II

Biological characteristics and tissue structure of a crustose coralline

Abstract

The disappearance of seaweed flora in some rocky areas, known as algal whitening, barren ground, coralline flats, or deforested areas, is associated with some species of coralline algae. To determine the biological characteristics of a representative species of crustose coralline alga, 18S rDNA gene was sequenced to identify the genus *Lithophyllum*. By morphological and distributional characteristics, it is deduced to *L. yessoense*. Measuring viability using triphenyl tetrazolium chloride showed highly viability from December to February. Cultural conditions of 16 °C, a 16 hr light:8 hr dark cycle, and 30 $\mu\text{E m}^{-2}\text{s}^{-1}$ light intensity were optimal for maintaining the viability of the alga for up to 5 days. The fatty acids included 9.7% ω -3 eicosapentaenoic acid. Scanning electron microscopy of the surface structure revealed round craters about 3.6 μm in diameter, covered with rough irregular and angular polygon-shaped structures about 1.0 to 3.7 μm in size. Biomimetic coralline alga based on the composition and structure might become an environmentally friendly antifouling material against the attachment of soft foulants.

Key words: Crustose alga, fatty acid, *Lithophyllum*, tissue structure, viability.

Introduction

Seaweeds play a major role in marine ecosystems. They provide nutrients for animals - either directly when fronds are eaten, or indirectly when decomposing parts break down into fine particles and are taken up by filter-feeding animals. Beds of seaweed provide shelter and habitat for scores of coastal animals for all or part of their lives. Coralline red algae, both of crustose (nongeniculate) and articulated corallines, abound in intertidal rocky shore areas and strongly influence the benthic community. Crustose coralline algae are a major calcifying component of the marine benthos from tropical to polar oceans at all depths within the photic zone (Steneck 1986). When the coralline algae are growing, the rock surfaces appear pink, while the fleshy seaweed flora disappears from the rocky areas. In marine environments, this phenomenon is generally called algal whitening, barren ground (Tokuda et al. 1994), coralline flats, or deforested areas. It is now recognized as a natural hazard adversely affecting marine ecosystems and damaging commercial fishing areas. Although biological (Agateuma et al. 1997; Kitamura et al. 1993; Whalan et al. 2012) and physical (Johnson and Mann 1986; Masaki et al. 1984) factors may be sufficient to prevent the recruitment of fleshy seaweeds, allelopathic bromoform (Ohsawa et al. 2001) and fatty acid (Kim et al. 2004; Luyen et al. 2009) substances may also inhibit the settlement or germination of seaweed spores. Consequently, coralline algae may prevent fouling by fleshy seaweeds. Alternatively,

biomimetic coralline alga material might become an environmentally friendly antifouling material. In nature, most coralline algae are pink and have almost indistinguishable shapes, those causes confusion in their identification. Therefore, in an attempt to make a biomimetic coralline alga material, we have to identify the species, select the best conditioned tissues as standard material, analyze the fatty acid composition, and observe the fine surface structure.

Materials and Methods

Plant material

Crustose coralline algae were collected monthly from the rocky intertidal area at Cheongsapo (35°09'28" N, 129°11'47" E), on the east coast of Busan, Korea. The samples were transported in a container with seawater to the laboratory. After rinsing well with autoclaved seawater to remove epiphytes and debris, the encrusted tissues were sonicated three times with 30-pulses of an ultrasonic water bath (low-intensity frequency of 90kHz) to remove other microepiphytes.

Molecular identification

Approximately 0.2 g of the coralline alga was chopped into very

tiny pieces and placed in a microtube. DNA was extracted using LiCl, following Hong et al. (1995). The 18S rDNA gene, encoding the ribosomal RNA in the small subunit of eukaryotic cytoplasmic ribosome, was amplified by polymerase chain reaction (PCR) with the universal primers 18sF (5' CAACCTGGTTGATCCTGCCAGT 3') and 18sR (5' GATCCTTCTGCAGGTTCACCTACGGAA 3') (Bird et al. 1992). The PCR cycling parameters consisted of 94°C for 5 min, 30 cycles of 94°C for 30 s, 57°C for 30 s, 72°C for 1.5 min, and a final 72°C for 10 min. The amplification products were sequenced using the same primers (SolGent, Daejeon, Korea). The sequences were edited and manipulated using MEGA3 (Kumar et al. 2004). Phylogenetic trees were inferred using the neighbor-joining algorithm (Saito and Nei, 1987) in MEGA3 with bootstrap analysis of 1,000 bootstrap replications.

Viability assay

To measure the viability of the coralline tissue, the assay of Park et al. (2006) was used. Briefly, 1 ml of 0.8% 2,3,5-triphenyltetrazolium chloride (TTC) in seawater containing 50 mM Tris-HCl buffer (pH 8.0) was added to 0.1 g of tissue in a 1.5-ml microtube and incubated in darkness for 1.5 hr at 20 °C under mineral oil. The triphenyl formazan that formed in the tissue was extracted with 0.6 ml of 0.2 N NaOH in 75% ethanol by heating for 15 min at 60 °C. The triphenyl formazan was quantified by measuring the absorbance at 475 nm. To determine the optimal conditions for maintaining viability, 0.25 g of the

tissue was cultured in 50 ml of seawater under $30 \mu\text{E m}^{-2}\text{s}^{-1}$ light intensity on a 16 h light:8 h dark cycle at 16 °C for 5 days as the standard conditions.

Scanning electron microscopy

Healthy tissue collected on February 9, 2012 was washed with Milli-Q water (Millipore, Billerica, MA) and dried under vacuum before scanning electron microscopy (SEM) analysis. For SEM images, tissues were mounted on conductive carbon tabs of a SEM post (Ted Pella, Inc., Redding, CA), sputter-coated using a Desk-II coater equipped with a gold target (Alfa Aesar, Ward Hill, MA), and imaged in a scanning-electron microscope (JSM-6700F; JEOL, Tokyo, Japan). To determine the elemental composition of parts of the tissues, the tissues were analyzed using energy-dispersive X-ray spectroscopy. The standards for carbon, oxygen, sodium, chlorine, and calcium were calcium carbonate, silicon dioxide, albite, potassium chloride, and wollastonite, respectively.

Fatty acid analysis

Fatty acids were determined by gas chromatographic quantification of their methyl esters (FAMEs), which were prepared using slightly modified method from the AOAC (2000). Total lipid was extracted from the dried samples using a Soxhlet extractor. Then,

FAMEs were prepared with 5 ml of methylation solution (1 H₂SO₄:20 CH₃OH:10 toluene) and heated at 100 °C for 1 h. Gas chromatography–mass spectroscopy (GC–MS) analysis was conducted using a 6890 network GC system with a 5973N Mass Selective Detector (MSD) (Agilent Technologies, Palo Alto, CA). The oven was started at 50 °C and held for 1 min, and then ramped up to 320 °C at 5 °C min⁻¹. The MSD was operated based on electron ionization.

Results

The group's internal taxonomy is still in a state of flux; molecular studies are proving more reliable than morphological methods in approximating relationships within the group (Bittner et al. 2011). To ascertain the species identification, we determined partial 18S rDNA gene sequence (Fig. 2-1). They were then aligned and analyzed using the neighbor-joining method to construct a dendrogram. The 1,391-bp 18S rDNA sequence from base 274 to 1,664 was compared to the sequences of 13 species of coralline algae obtained from the NCBI database to infer the phylogenetic relationship (Fig. 2-2). The 18S rDNA sequence showed the closest to the sequence of *Lithophyllum incrustans*. The sequence matched 99% homology with 15 base difference from the *L. incrustans* sequence (GenBank accession # AF093410.1). Meanwhile, the *L. incrustans* is described as thick, dull

chalky, yellowish, pink or lavender calcareous crusts forming irregular concretions, to 40 mm thick, margins ridged where crusts meet, in the AlgaeBase (Guiry and Guiry, 2013). The alga used in this study has typically no margins ridged where crusts meet, and is not much thick, dull chalky and yellowish. Thus, the alga was identified to be belonging to the crustose coralline *Lithophyllum* genus using the 18S rDNA sequence, but not able to confirm the species level. By the morphological shape, the crustaceous thalli spread irregularly like a pinky patch, non-verrucose on surface. It is distributed in warm current sea along the coasts of Jeju and Busan, Korea. From the morphological and distributional characteristics, it maybe deduced to *L. yessoense* (Tokuda et al. 1994). Using the TTC method, we measured the viability of crustose coralline tissues collected at the same site throughout the year (Fig. 2-3) and quantified viability as the absorbance at 475 nm. The tissues collected in February had the greatest viability, which then decreased gradually in the spring and summer. Some tissues remained pinky crust, and some disappeared from the rock surface. In autumn, they started to grow, and most tissues recovered their viability. In December and February, the tissues again had the healthiest pink structure and greatest viability. Therefore, this period would be the best season to use as a model structure of a biomimetic antifouling material. To keep healthy tissues, we optimized the maintenance conditions using the TTC viability assay (Fig. 2-4). The optimal temperature for incubation was 16 °C, the optimal light intensity was 30 $\mu\text{E m}^{-2}\text{s}^{-1}$ with white fluorescent

light, and the optimal light period was a 16 h light:8 h dark cycle. Under these conditions, the tissues maintained the best viability for up to 5 days in a standing flask containing natural seawater. Therefore, the tissues were kept at the optimized conditions and used within 5 days. We determined the major fatty acid composition of healthy coralline tissue (Table 2-1). Of the fatty acids, 23.4% were PUFAs, with ω -3 eicosapentaenoic acid (EPA; C20:5) comprising 9.7% and ω -6 arachidonic acid (AA; C20:4) comprising 5.1%; the ω -6: ω -3 ratio was 1.42. In the previous study (Luyen et al. 2009), EPA and AA showed strong lytic activity against algal spore with LC_{50} =2.1 and 1.8 μ g/ml, respectively. Therefore, the preparation of biomimetic calcium carbonate nanoparticles with EPA and/or AA will have potent antifouling activity as an environmentally friendly bio-control. The surface structure of the crustose coralline tissue was examined using SEM. The tissue surface was covered with round craters about 2.5 to 5.0 μ m in diameter at the surface (Fig. 2-5A). Most of these crater-shaped structures were irregular circles of average 3.6 μ m in diameter. The upper rough tissue was covered with irregular and angular polygon-shaped structures about 1.0 to 3.7 μ m in size (Fig. 2-5B). The average is about 2.1 μ m in size. SEM-based energy-dispersive X-ray spectroscopy showed that the relative elemental composition was 50% carbon, 39% oxygen, 3% sodium, 2% chlorine, and 6% calcium by atomic percentage, or 37% carbon, 38% oxygen, 5% sodium, 5% chlorine, and 15% calcium by weight.

Discussion

A dominant crustose coralline alga from barren grounds was pinkish to reddish and generally characterized by their encrusted calcareous composition. They typically colonized rocky substrates and formed smooth and flat crust in the intertidal area exposed to waves. It is known that many areas of the rocky shorelines of Korea and Japan are dominated by crustose coralline algae such as *Lithophyllum yessoense* Foslie (Kim 2000; Suzuki et al. 1998). The group's internal taxonomy is still in a state of flux; molecular studies are proving more reliable than morphological methods in approximating relationships within the group (Bittner et al. 2011). Among the factors preventing the settlement or germination of fleshy seaweed spores, we found that polyunsaturated fatty acids (PUFAs) have potent lytic activity against algal spores (Luyen et al. 2009). When preparing biomimetic coralline alga material, the antifouling activity might be enhanced by adding bioactive PUFAs. Of the fatty acids from healthy coralline tissue, 9.7% were ω -3 eicosapentaenoic acid (EPA; C20:5) and 13.7% were the other PUFAs. In a previous study, EPA showed strong lytic activity against algal spore with $LC_{50}=2.1 \mu\text{g ml}^{-1}$ (Luyen et al. 2009). Therefore, the preparation of biomimetic calcium carbonate nanoparticles with EPA might have potent antifouling activity as an environmentally friendly biocontrol. Some corallines slough off a surface layer of epithelial cells, which in a few cases may be an antifouling mechanism which serves the same function as enhancing

herbivore recruitment (Johnson and Mann 1986; Madaki et al. 1984). This also affects the community, as many algae recruit on the surface of a sloughing coralline, and are then lost with the surface layer of cells. This can also generate patchiness within the community. Sloughing in this case is probably a means of eliminating old reproductive structures and grazer-damaged surface cells, and reducing the likelihood of surface penetration by burrowing organisms.

The major mineral content was calcium carbonate. Calcification by crustose coralline algae is crucial to the formation and maintenance of coral reefs (Littler 1972). Coralline algae bind adjacent substrata and provide a calcified tissue barrier against erosion. They also serve as food for grazers – notably parrot fish, urchins, and starfish (Adey 1998). Coralline algae provide hard substrata for settlement and metamorphosis in a large diversity of marine invertebrate larvae, including abalone (Roberts et al. 2004) We found that allelopathic fatty acid substances prevented the settlement or germination of fleshy seaweed spores (Kim et al. 2004; Luyen et al. 2009). Bromomethane released by the articulated coralline alga can eliminate epiphytic organisms, especially microalgae on the surface, and might induce the continuation of coralline flats in marine environments (Ohsawa et al. 2001). Crustose coralline algae are thus capable of limiting the local abundance of fleshy seaweed by reducing recruitment success. Furthermore, biomimetic materials derived from the crustose coralline algae, containing antifouling substances, might be developed to protect against the attachment of soft foulants, especially micro- and

macroalgae.

Calcification by crustose coralline algae is crucial to the formation and maintenance of coral reefs (Littler 1972). Coralline algae bind adjacent substrata and provide a calcified tissue barrier against erosion. They also serve as food for grazers – notably parrot fish, urchins, and starfish (Adey 1998). Coralline algae provide hard substrata for settlement and metamorphosis in a large diversity of marine invertebrate larvae, including abalone (Roberts et al. 2004) We found that allelopathic fatty acid substances prevented the settlement or germination of fleshy seaweed spores (Kim et al. 2004; Luyen et al. 2009). Bromomethane released by the articulated coralline alga can eliminate epiphytic organisms, especially microalgae on the surface, and might induce the continuation of coralline flats in marine environments (Ohsawa et al. 2001). Crustose coralline algae are thus capable of limiting the local abundance of fleshy seaweed by reducing recruitment success. Furthermore, biomimetic materials derived from the crustose coralline algae, containing antifouling substances, might be developed to protect against the attachment of soft foulants, especially micro- and macroalgae.

5' GTTCAAATTTCTGACCTATCAACTTTTCGATGGTAAGGTAGTGTCTTACCATGGTGGTAAC
 GGGTAACGGACCGTGGGTGCGGGACTCCGGAGAGGGAGCCTGAGAAAACGGCTACCACATCCA
 AGGAAGGCAGCAGGCGCGCAACTTACCCAATCCAGACTCTGGGAGGTAGTGACAAGAAATAT
 CAATAGGGGAGCCTA*TGGTTCTTCTAATTGGAATGAGATCGAGCTAAACAGCCATATCGAGA*
 ATCCAGCAGAGGGCAAGTCTGGTGCCAGCAGCCGCGTAATTCCAGCTCTGTAAGCGTATAC
 CAAAGTTGTTGCAGTTAAAACGCTCGTAGTCGGACTTTGGCAGTTCCGGGAGTGTGCGCGTC
 GTGTGCACGCTTTGCGGGGACTGCTTTTTGTGGTATTGCGTGGGATGAAGCATTTTTTATTAAT
 GAACGTCCCTCCGCAACCACTTTTTACTGTGAGAAAATCAGAGTGCTCAAAGCAGGCATTTG
 CCGTGAATGTATTAGCATGGAATAATAGAATAGGACTT*GTTTCTATTTTTGTTGGTTTTGTTGG*
 GAATGAGTAATGATTAAGAGGGACAGTTGGGGGTATTTGTATTTTCGGCGCTAGAGGTGAAA
 TTCTTAGATTGCCGAAAGACAACTGCTGCGAAAGCGTCTACCAAGGATGTTTTTCATTGATC
 AAGAACGAAAGTAAGGGGATCGAAGACGATCAGATACCGTCGTAGTCTTTACTATAAACGAT
 GAGGACTGGGGATCGGGCGAGGCATTACGATGACCCGCCCGGCACCCTTCGAGAAATCAAAG
 TGTTTGCTTTCTGGGGGAGTATGGTCGCAAGTCTGAACTTAAAGGAATTGACGGAAGGGC
 ATCACCGGGTGTGGAGCCTGCGGCTTAATTTGACTCAACACGGGAAAACCTTACCAGGTCAGG
 ACATAGTGAGGATTGACAGATTGAGAGCTCTTTCTTGATTCTATGGTTGGTGGTGCATGGCC
 GTTCTTAGTTGGTGGAGTGATTTGTCTGGTTAATTCGTTAACGAGCGAGACCTGGGCGTGC
 TAACTAGGGGGTACTACCATTTTTGGTAGTATACTTCCCTTCTTAGACGGACTGTGGGCGTCT
 AGCCACGGAAGCTCCAGGCAATAACAGGTCTGAGATGCCCTTAGATGTTCTGGGCCGCACG
 CGTGCTACACTGAGTGGATCAGCGGGTTAGGTAACGCGAAAGTGTGTCCTAATCTTCAAATC
 CGCTCGTGATGGGGATTGACGGTTGCAATTTTCCGTCATGAACGAGGAATACCTTGTAGGCG
 CGTTTCATCATAACGCGCCGAATACGTCCCTGCCCTTTGTACACACCGCCCGTGCCTCCTAC
 CGATTGAGTGGTCCGGTGAGGCTTTGGGA3'

Figure 2-1. 18S rDNA sequence (1391 base) of the crustose coralline alga. Different parts of sequence from the *Lithophyllum incrustans* (GenBank accession # AF093410.1) are in italic letters.

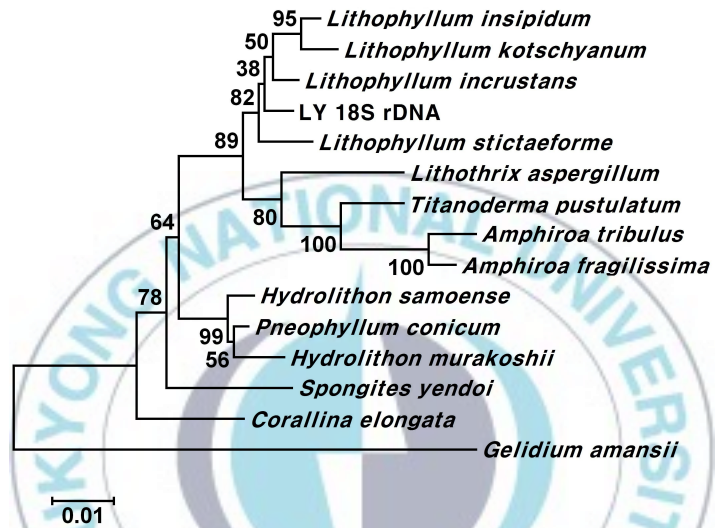


Figure 2-2. Phylogenetic dendrograms of the crustose coralline alga based on 18S rDNA sequence, and constructed using the neighbor-joining method. Numbers at nodes indicate the level of bootstrap support (1,000 replicates).

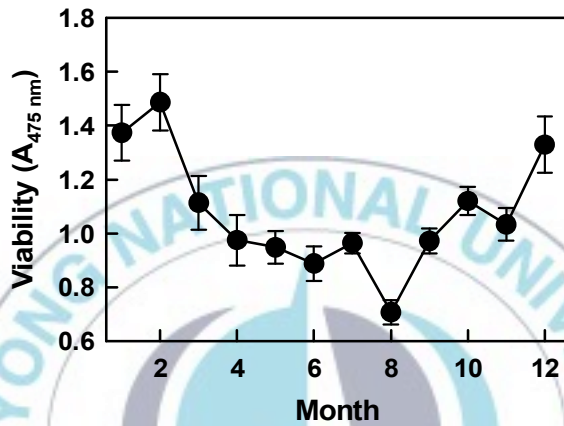


Figure 2-3. Seasonal variation in the viability of the crustose coralline tissue. The viability was quantified using the absorbance at 475 nm, and the values are the mean \pm SD of at least five independent assays.

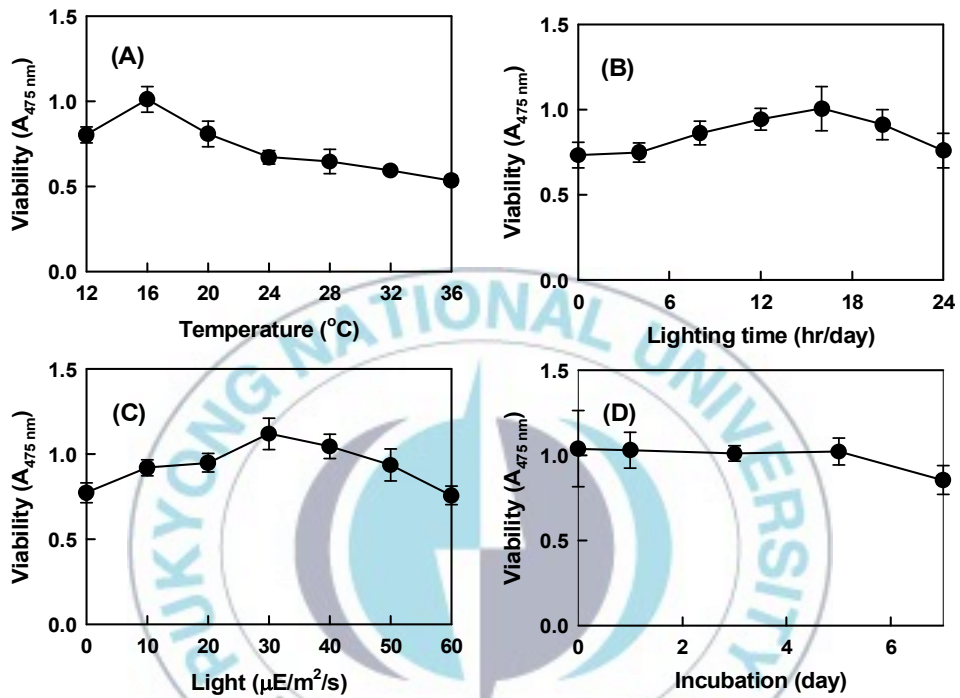


Figure 2-4. Effect of various parameters on the optimal maintenance of the crustose coralline tissue: (A) incubation temperature, (B) amount of light per day, (C) light intensity, and (D) incubation period under the optimized conditions. The viability was measured using the absorbance at 475 nm, and the values are expressed as the mean \pm SD of at least five independent assays.

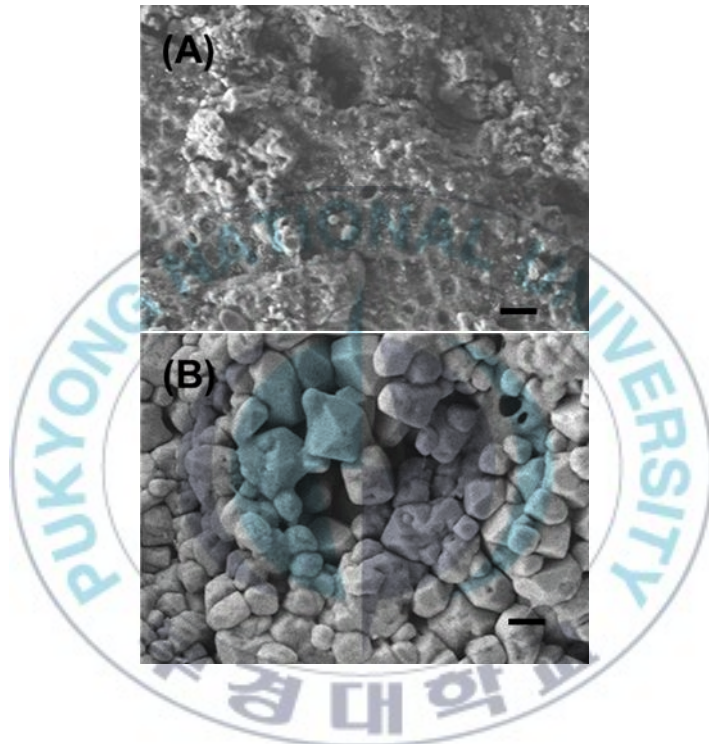


Figure 2-5. Tissue of the articulated coralline alga. Scanning electron micrograph of the coralline tissue by 1,000 (A) and 5,000 (B) magnitude. The bars in A and B indicate 10 μm and 2 μm , respectively.

Table 2-1. Profile of the major fatty acids (% of total fatty acids) in the crustose coralline tissue collected on February 9, 2012.

Fatty acids	Relative amount (%)
C16:0	36.9
C18:0	11.6
C18:1 ω -9	1.2
C18:2 ω -6	3.2
C18:3 ω -6	1.5
C20:0	1.7
C20:4 ω -6	5.1
C20:5 ω -3	9.7
C22:0	11.4
C22:2 ω -6	3.2
C24:0	3.3
Saturated fatty acids	74.0
MUFAs	2.6
PUFAs	23.4

Reference

- Adey WH. 1998. Coral reefs: algal structured and mediated ecosystems in shallow, turbulent, alkaline waters. *J Phycol* 34: 393-406.
- Agateuma Y, Mateuyama K, Nakata A, Kawai T, Nishikawa N. 1997. Marine algal succession on coralline flats after removal of sea urchins in Suttsu bay on the Japan Sea coast of Hokkaido, Japan. *Nippon Suisan Gakkaishi* 63: 672-680.
- AOAC. 2000. *Official Methods of Analysis*. Vol. II, 17th ed. Association of Official Analytical Chemists, Washington, D.C., USA.
- Bird CJ, Rice EL, Murphy CA, Ragan MA. 1992. Phylogenetic relationships in the Gracilariales (Rhodophyta) as determined by 18S rDNA sequences. *Phycologia* 31: 510-522.
- Bittner L, Payri CE, Maneveldt GW, Couloux A, Cruaud C, de Riviers B, Le Gall L. 2011. Evolutionary history of the Corallinales (Corallinophycidae, Rhodophyta) inferred from nuclear, plastidial and mitochondrial genomes. *Mol Phylogenet Evol* 61: 697-713.
- Guiry MD, Guiry GM. 2013. *AlgaeBase*. World-wide electronic publication, National University of Ireland, Galway. <http://www.algaebase.org;searchedon22January2013>.
- Hong YK, Kim SD, Polne-Fuller M, Gibor A. 1995. DNA extraction conditions from *Porphyra perforata* using LiCl. *J Appl Phycol* 7: 103-107.

- Johnson CR, Mann KH. 1986. The crustose coralline alga, *Phymatolithon* Foslie, inhibits the overgrowth of seaweeds without relying on herbivores. *J Exp Mar Biol Ecol* 96: 127-146.
- Kim JH. 2000. Taxonomy of the Corallinales, Rhodophyta, in Korea. Ph.D. dissertation, Seoul National University, Seoul, Korea.
- Kim MJ, Choi JS, Kang SE, Cho JY, Jin HJ, Chun BS, Hong YK. 2004. Multiple allelopathic activity of the crustose coralline alga *Lithophyllum yessoense* against settlement and germination of seaweed spores. *J Appl Phycol* 16: 175-179.
- Kitamura H, Kitahara S, Koh HB. 1993. The induction of larval settlement and metamorphosis of two sea urchins, *Pseudocentrotus depressus* and *Anthocidaris crassispina*, by free fatty acids extracted from the coralline red algae *Corallina pilulifera*. *Mar Biol* 115: 387-392.
- Kumar S, Tamura K, Nei M. 2004. MEGA3: integrated software for molecular evolutionary genetic analysis and sequence alignment. *Brief Bioinform* 5: 150-163.
- Littler MM. 1972. The crustose Corallinaceae. *Oceanogr Mar Biol Annu Rev* 10: 311 - 347.
- Luyen QH, Cho JY, Choi JS, Kang JY, Park NG, Hong YK. 2009. Isolation of algal spore lytic C17 fatty acid from the crustose coralline seaweed *Lithophyllum yessoense*. *J Appl Phycol* 21: 423-427.
- Masaki T, Fujita D, Hagen NT. 1984. The surface ultrastructure and

epithallium shedding of crustose coralline algae in an Isoyake area of southwestern Hokkaido, Japan. *Hydrobiologia* 116/117: 218-223.

Ohsawa N, Ogata Y, Okada N, Itoh N. 2001. Physiological function of bromoperoxidase in the red marine alga, *Corallina pilulifera*: production of bromoform as an allelochemical and the simultaneous elimination of hydrogen peroxide. *Phytochemistry* 58: 683-692.

Park SM, Kang SE, Choi JS, Cho JY, Yoon SJ, Ahn DH, Hong YK. 2006. Viability assay of coralline algae using triphenyltetrazolium chloride. *Fish Sci* 72: 912-914.

Roberts RD, Kaspar HF, Barker RJ. 2004. Settlement of abalone larvae in response to five species of coralline algae. *J Shellfish Res* 23: 975-987.

Saito N, Nei M. 1987. The neighbor-joining method: a new method for reconstructing phylogenetic tree. *Mol Biol Evol* 4: 406-425.

Steneck RS. 1986. The ecology of coralline algal crusts: convergent patterns and adaptive strategies. *Annu Rev Ecol Syst* 17: 273 - 303.

Suzuki Y, Takabayashi T, Kawaguchi T, Matsunaga K. 1998. Isolation of an allelopathic substance from the crustose coralline algae, *Lithophyllum* spp., and its effect on the brown alga, *Laminaria religiosa* Miyabe (Phaeophyta). *J Exp Mar Biol Ecol* 225: 69-77.

Tokuda H, Kawashima S, Ohno M, Ogawa H. 1994. *Seaweeds of*

Japan. Midori Shobo Co., Tokyo, Japan.

Whalan S, Webster NS, Negri AP. 2012. Crustose coralline algae and a cnidarian neuropeptide trigger larval settlement in two coral reef sponges. PLoS ONE 7, e30386.



Chapter III

Biological characteristics and tissue structure of the branched coralline alga *Corallina pilulifera*

Abstract

The decrease in the seaweed flora in some rocky areas, known as algal whitening or barren ground, is associated with some species of coralline algae. To determine the biological characteristics of a representative species of branched coralline alga, the number of medullary tiers was counted and ranged from 12 to 16. The 18S rDNA, *psbA*, and *rbcL* genes were used to confirm the identification of *Corallina pilulifera*. Measuring viability using triphenyl tetrazolium chloride showed highly viability from December to January. Cultural conditions of 16 °C, a 16 h light:8 h dark cycle, and 40 $\mu\text{E m}^{-2}\text{s}^{-1}$ light intensity were optimal for maintaining the viability of the coralline alga for up to 3 days. The fatty acids included 31.4% ω -3 eicosapentaenoic acid. Scanning electron microscopy of the surface structure revealed unique round wells about $7.9 \pm 1.3 \mu\text{m}$ in diameter.

Key words: *Corallina pilulifera*, fatty acid, tissue structure, viability.

Introduction

Seaweed is an important source of food and shelter; its biomass takes up carbon in marine environments, and it is a source of chemicals for commercial applications (Thomas 2002). Coralline red algae abound in nearshore areas and strongly influence the benthic community. When coralline algae are growing, the rock surfaces appear pink, while the fleshy seaweed flora disappears from the rocky areas. In marine environments, this phenomenon is generally called algal whitening, barren ground (Tokuda et al. 1994), coralline flats, or deforested areas. It is now recognized as a natural hazard adversely affecting marine ecosystems and damaging commercial fishing areas. Although biological (Kitamura et al. 1993; Agateuma et al. 1997) and physical (Masaki et al. 1984; Johnson and Mann 1986) factors may be sufficient to prevent the recruitment of fleshy seaweeds, allelopathic bromoform (Ohsawa et al. 2001) and fatty acid (Kim et al. 2004; Luyen et al. 2009) substances may also inhibit the settlement or germination of seaweed spores. Consequently, coralline algae may also prevent fouling by fleshy seaweeds. Alternatively, biomimetic coralline alga material might become an environmentally friendly antifouling material. In nature, most coralline algae are pink and have almost indistinguishable shapes. Seasonal changes in articulated coralline algae can also cause confusion in their identification. Therefore, in an attempt to make a biomimetic coralline alga material, we first had to identify the species, select the best conditioned tissues as standard

material, analyze the fatty acid composition, and observe the fine surface structure.

Materials and Methods

Plant material

Coralline algae were collected monthly from the rocky intertidal area at Cheongsapo (35°09'28" N, 129°11'47" E), on the east coast of Busan, Korea. The samples were transported in a container with seawater to the laboratory. After rinsing well with autoclaved seawater to remove epiphytes and debris, the tissues were sonicated three times with 30-s pulses of an ultrasonic water bath (low-intensity frequency of 90 kHz) to remove other microepiphytes.

Medullary tier

The coralline algae were fixed in SUSA solution (4.5 g HgCl₂, 0.5g NaCl, 20 ml 40% formalin, 4 ml trichloroacetic acid, and 80 ml distilled water) for 12h and then transferred to formalin solution for 24h. The fronds were fixed for another 24h in 10% neutral buffered formalin solution (100 ml 40% formaldehyde, 800 ml distilled water, 4.0g NaH₂PO₄, and 6.5g anhydrous Na₂HPO₄). The tissues were

dehydrated through an alcohol series from 70% to 100% and cleaned with three changes of xylene. Specimens embedded in paraffin wax were cut at 5 μ m thickness with a rotary type microtome (Reichert–Jung 820; Leica, Wetzlar, Germany) and stained with hematoxylin and eosin (Clark 1981).

Molecular identification

Approximately 0.2 g of the coralline alga was chopped into very tiny pieces and placed in a microtube. DNA was extracted using LiCl, following Hong et al. (1995). The 18S rDNA gene, encoding the ribosomal RNA in the small subunit of eukaryotic cytoplasmic ribosome, was amplified by polymerase chain reaction (PCR) with the universal primers 18sF (5' CAACCTGGTTGATCCTGCCAGT 3') and 18sR (5' GATCCTTCTGCAGGTTACCTACGGAA 3') (Bird et al. 1992). The *psbA* gene encoding the D1 protein of the photosystem II reaction center complex in the photosynthetic organ was amplified by PCR with the primers *psbAF* (5' ATTGCATTCGTTGCTGCTCCTC 3') and *psbAR* (5' GTGAACCAGATTTCCTACTACAGGC 3') (Kim et al. 2006). The *rbcL* gene, known as RuBisCO or ribulose-1,5-bisphosphate carboxylase/oxygenase in photosynthesizing chloroplasts, was amplified by PCR with the primers *rbcLF* (5' GCAGGTGAATCATCTACAGCAAC 3') and *rbcLR* (5' GCTTGAATACCGTCTGGATGACC 3') (Freshwater et al. 1994). The PCR cycling parameters consisted of 94 °C for 5 min, 30 cycles of 94 °C for 30 s, 57 °C for 30 s, 72 °C for 1.5 min, and a

final 72 °C for 10 min. The amplification products were sequenced using the same primers (SolGent, Daejeon, Korea). The sequences were edited and manipulated using MEGA3 (Kumar et al. 2004). Phylogenetic trees were inferred using the neighbor-joining algorithm (Saito and Nei 1987) in MEGA3 with bootstrap analysis of 1,000 bootstrap replications.

Viability assay

To measure the viability of the coralline tissue, the assay of Park et al. (2006) was used. Briefly, 1 ml of 0.8% 2,3,5-triphenyltetrazolium chloride (TTC) in seawater containing 50 mM Tris-HCl buffer (pH 8.0) was added to 0.05 g of tissue in a 1.5-ml microtube and incubated in darkness for 1.5 h at 20 °C under mineral oil. The triphenyl formazan that formed in the tissue was extracted with 0.6 ml of 0.2 N NaOH in 75% ethanol by heating for 15 min at 60 °C. The triphenyl formazan was quantified by measuring the absorbance at 475 nm. To determine the optimal conditions for maintaining viability, 0.25 g of the tissue was cultured in 50 ml of seawater under 40 $\mu\text{E m}^{-2}\text{s}^{-1}$ light intensity on a 16 h light:8 h dark cycle at 16 °C for 3 days as the standard conditions.

Scanning electron microscopy

Healthy tissue collected on January 11, 2012 was washed with

Milli-Q water (Millipore, Billerica, MA) and dried under vacuum before scanning electron microscopy (SEM) analysis. For SEM images, tissues were mounted on conductive carbon tabs of a SEM post (Ted Pella, Inc., Redding, CA), sputter-coated using a Desk-II coater equipped with a gold target (Alfa Aesar, Ward Hill, MA), and imaged in a scanning-electron microscope (JSM-6700F; JEOL, Tokyo, Japan). To determine the elemental composition of parts of the tissues, the tissues were analyzed using energy-dispersive X-ray spectroscopy. The standards for carbon, oxygen, and calcium were calcium carbonate, silicon dioxide, and wollastonite, respectively.

Fatty acid analysis

Fatty acids were determined by gas chromatographic quantification of their methyl esters (FAMEs), which were prepared using slightly modified method from the AOAC (2000). Total lipid was extracted from the dried samples using a Soxhlet extractor. Then, FAMEs were prepared with 5 ml of methylation solution (1 H₂SO₄:20 CH₃OH:10 toluene) and heated at 100 °C for 1 h. Gas chromatography-massspectroscopy (GC-MS) analysis was conducted using a 6890 network GC system with a 5973N Mass Selective Detector (MSD) (Agilent Technologies, Palo Alto, CA). The oven was started at 50 °C and held for 1 min, and then ramped up to 320 °C at 5 °C min⁻¹. The MSD was operated based on electron ionization.

Results

Eight samples of dominant coralline algae from different barren grounds and different seasons were collected. They were pinkish to reddish with a whitish apex and were generally characterized by their calcareous composition (Figure 3-1A). They typically colonized rocky substrates and formed turfs in the intertidal area exposed to waves. The number of medullary tiers per intergeniculum and other characters were observed after staining with hematoxylin and eosin (Figure 3-1B). The number of tiers of medullary cells per intergeniculum was between 12 and 16. The intergenicular length was approximately 1.0 - 1.4 mm. The alga had pinnate fusing branches that were somewhat fan-shaped, with broad intergenicula, and were truncated at the ends. The main base of the branch was almost as wide as it was long and the branches were somewhat subspherical. The frond height ranged from 3 to 7 cm. To ascertain the species identification, we determined partial 18S rDNA, *psbA*, and *rbcL* gene sequences. They were then aligned and analyzed using the neighbor-joining method to construct a dendrogram. The 1,156-bp 18S rDNA sequence from base 412 to 1,567 was compared to the sequences of 20 species of coralline algae obtained from the NCBI database to infer the phylogenetic relationships (Figure 3-2A). The 18S rDNA sequence had 99% homology with the *Corallina* sp. sequence (GenBank accession # FM180100.1). Similarly, the 881-bp *psbA* plastid gene sequence from base 31 to 911 was compared with the sequences of 14 species of

coralline algae obtained from the NCBI database (Figure 3-2B). The *psbA* gene sequence shared 100% homology with the *C. pilulifera* sequence (GenBank accession # DQ787634.1). Likewise, the 943-bp *rbcl* plastid gene sequence from base 226 to 1,168 (Figure 3-2C) shared 100% homology with the *C. pilulifera* sequence (GenBank accession # DQ787558.1). Therefore, the species was identified as the articulated coralline alga *C. pilulifera* using 18S rDNA, *psbA*, and *rbcl* gene identification. Using the TTC method, we measured the viability of *C. pilulifera* tissues collected at the same site throughout the year (Figure 3-3) and quantified viability as the absorbance at 475 nm. The tissues collected in January had the greatest viability, which then decreased gradually in the spring. Some tissues remained short or as unbranched fronds, and some disappeared from the rock surface. In late spring and summer, new buds appeared on epilithic basal crusts. In autumn, they started to grow, and most tissues recovered their viability. In December and January, the tissues again had the healthiest pink structure and greatest viability. Therefore, this period would be the best season to use as a model structure of a biomimetic antifouling material. To keep healthy tissues, we optimized the maintenance conditions using the TTC viability assay (Figure 3-4). The optimal temperature for incubation was 16 °C, the optimal light intensity was 40 $\mu\text{E m}^{-2}\text{s}^{-1}$ with white fluorescent light, and the optimal light period was a 16 h light:8 h dark cycle. Under these conditions, the tissues maintained the best viability for up to 3 days in a standing flask containing natural seawater. Therefore, the tissues

were kept at the optimized conditions and used within 3 days. We determined the major fatty acid composition of healthy *C. pilulifera* tissue (Table 3-1). Of the fatty acids, 45.4% were PUFAs, with ω -3 eicosapentaenoic acid (EPA; C20:5) comprising 31.4%; the ω -6: ω -3 ratio was 0.45. The surface structure of the coralline tissue was examined using SEM. The tissue surface was covered with unique round wells about $7.9 \pm 1.3 \mu\text{m}$ in diameter at the surface (Figure 3-5). Most of these well-shaped structures were irregular circles, forming cones vertically. SEM-based energy-dispersive X-ray spectroscopy showed that the relative elemental composition was 33% carbon, 56% oxygen, and 11% calcium by atomic percentage, or 23% carbon, 53% oxygen, and 24% calcium by weight.

Discussion

The species *Corallina pilulifera* was identified using anatomical characters, such as the tier number per intergeniculum (12 - 16) and intergenicular length (0.9 - 1.2 mm; Baba et al. 1988; Akioka et al. 1999). All eight samples of the coralline algae collected had the same range of tier numbers, which is a key character of *C. pilulifera*. Slight differences in the intergenicular length, width, frond height, branch, conceptacle, and intergenicular shapes were seen. Guiry and Guiry (2012) included four varieties of *C. pilulifera* and 29 entries of *C. officinalis* in AlgaeBase that were classified as uncertain. Morphological

studies alone no longer suffice to identify species, as demonstrated by the apparent duplication of descriptions due to geographical, seasonal, and environmental differences. Differences in microhabitat conditions, such as desiccation, epiphyte loading, and the abundance of herbivores, can also alter the morphology (Akioka et al. 1999). Therefore, we used molecular information to complement the physical variation. Molecular analysis based on 18S rDNA has been used to elucidate the division of Corallinoideae (Walker et al. 2009), the classification of the order Corallinales with 35 species of coralline algae (Bailey and Chapman, 1998), and the relationships within the tribe Janieae (Kim et al. 2007). The evolutionary history of the Corallinales has also been inferred from nuclear, plastidial, and mitochondrial genomes (Bittner et al. 2011). Among the factors preventing the settlement or germination of fleshy seaweed spores, we found that polyunsaturated fatty acids (PUFAs) have potent lytic activity against algal spores (Luyen et al. 2009). When preparing biomimetic coralline alga material, the antifouling activity might be enhanced by adding bioactive PUFAs. Of the fatty acids from healthy *C. pilulifera* tissue, 31.4% were ω -3 eicosapentaenoic acid (EPA; C20:5) and 14% were the other PUFAs. In a previous study, EPA showed strong lytic activity against algal spore with $LC_{50}=2.1 \mu\text{g ml}^{-1}$ (Luyen et al. 2009). Therefore, the preparation of biomimetic calcium carbonate nanoparticles with EPA might have potent antifouling activity as an environmentally friendly biocontrol. The mineral content of *C. pilulifera* was 0.13% sodium, 1.75% chloride, 4.37% magnesium, 18.4% calcium, 0.31% iron, and 28.5% carbonate

(Yan 1999). These high levels of essential minerals, especially magnesium, calcium, and iron, coupled with the low sodium, chloride, and potassium contents, make this species a potential mineral source for livestock.

Corallina pilulifera is an articulated coralline alga with a hard, abrasive calcareous skeleton. It dominates the intertidal zone on rocky substrate where strong waves occur. It produces a bromoperoxidase that acts on bromide and iodide, and is potentially useful as a catalyst for biotransformation (Itoh et al. 1985). The allelopathic bromomethane released by the alga can eliminate epiphytic organisms, especially microalgae on the surface, and might induce the continuation of coralline flats in marine environments (Ohsawa et al. 2001). The growth of the red tide microalga *Prorocentrum donghaiense* was inhibited by aqueous and methanolic extracts of *C. pilulifera* (Wang et al. 2007). The methanolic extract also had an antioxidant protective effect on UVA-induced oxidative stress in human fibroblasts (Ryu et al. 2009). The ethanol extract inhibited the growth of the HeLa cancer cell line and induced apoptosis in a dose-dependent manner (Kwon et al. 2007). It can be used as a source of essential minerals for livestock or agriculture (Yan 1999). Furthermore, antifouling substances or biomimetic materials derived from *C. pilulifera* might be developed to protect against the attachment of soft foulants, especially micro- and macroalgae.

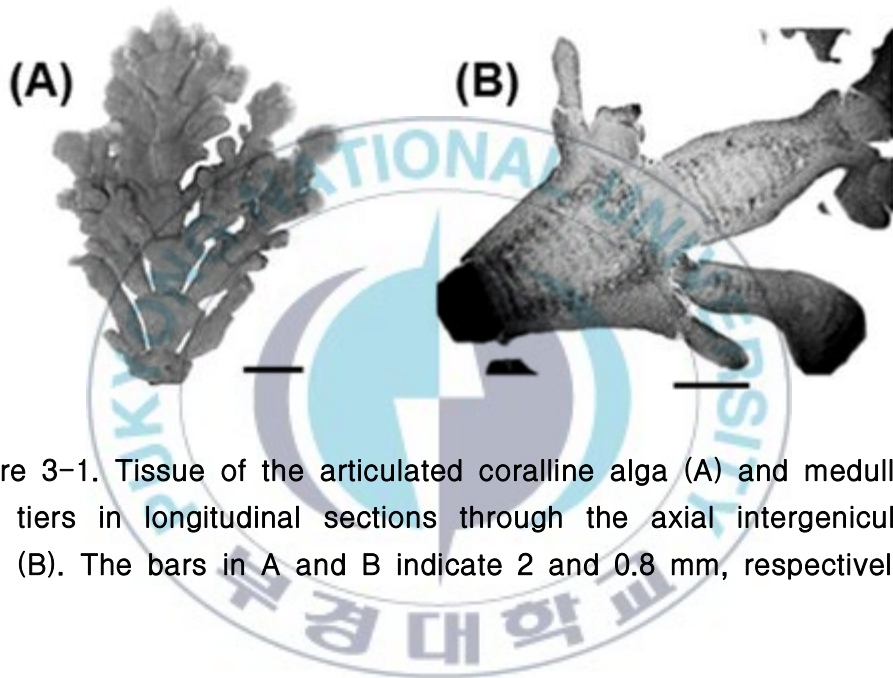


Figure 3-1. Tissue of the articulated coralline alga (A) and medullary tiers in longitudinal sections through the axial intergeniculum (B). The bars in A and B indicate 2 and 0.8 mm, respectively.

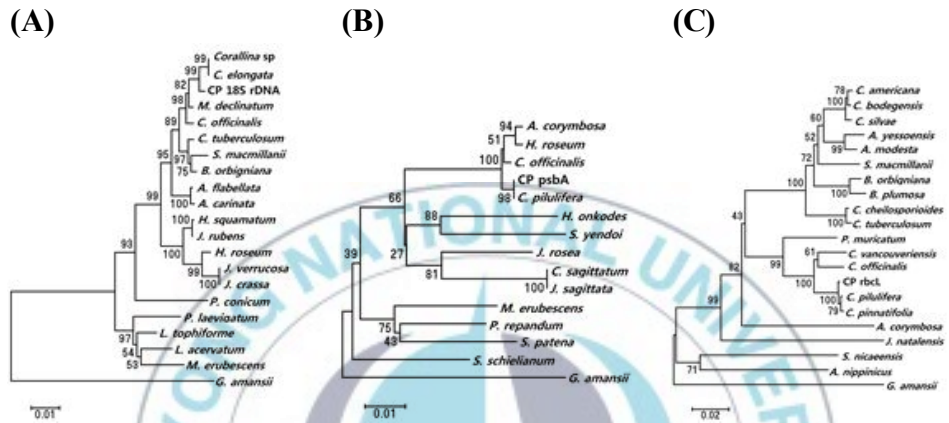


Figure 3-2. Phylogenetic dendrograms of the coralline alga (CP) based on 18S rDNA (A), psbA (B), and rbcL (C) sequences, and constructed using the neighbor-joining method. Numbers at nodes indicate the level of bootstrap support (1,000 replicates).

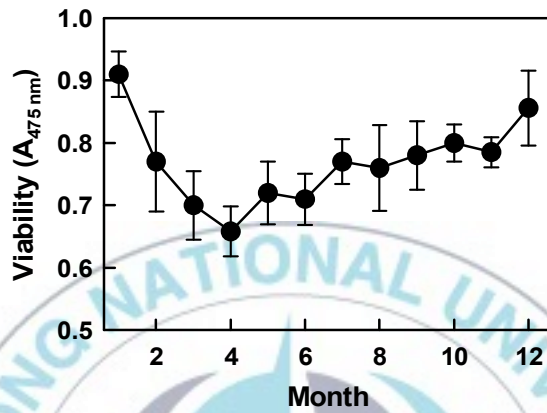


Figure 3-3. Seasonal variation in the viability of *Corallina pilulifera* tissue. The viability was quantified using the absorbance at 475 nm, and the values are the mean \pm s.d. of at least five independent assays.

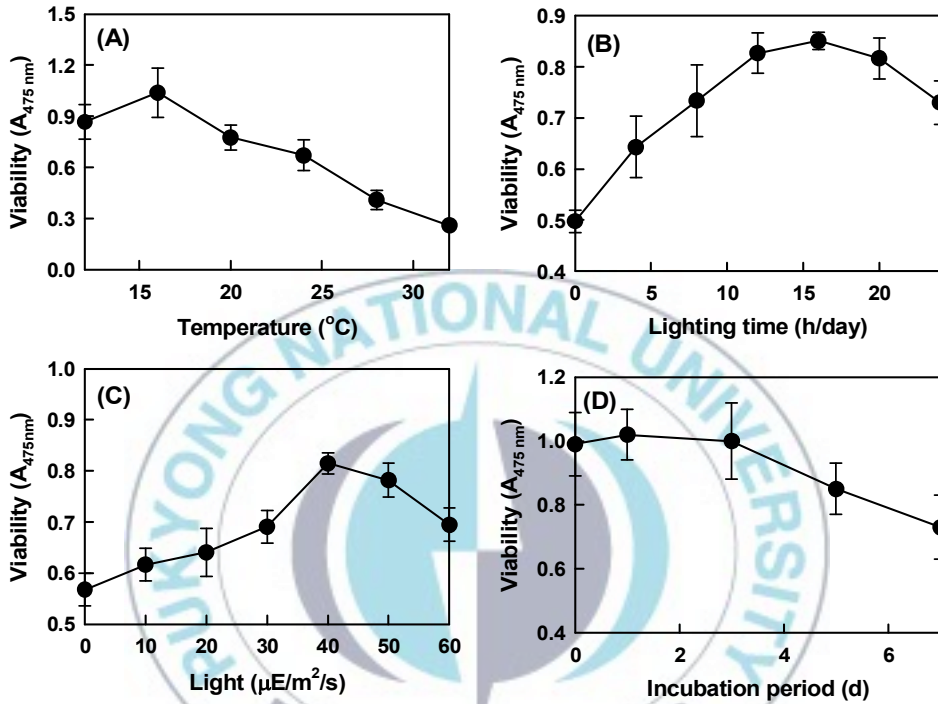


Figure 3-4. Effect of various parameters on the optimal maintenance of *Corallina pilulifera* tissue: (A) incubation temperature, (B) amount of light per day, (C) light intensity, and (D) incubation period under the optimized conditions. The viability was measured using the absorbance at 475 nm, and the values are expressed as the mean \pm SD of at least five independent assays.

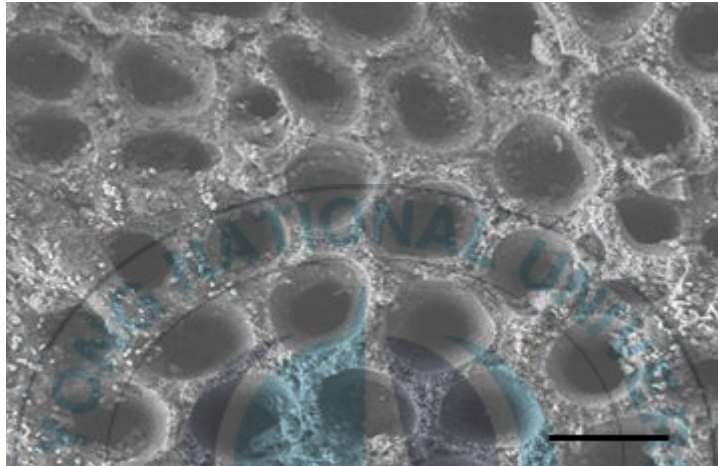


Figure 3-5. Scanning electron micrograph of *Corallina pilulifera* tissue. Bar = 10 μm .

Table 3-1. Profile of the major fatty acids (% of total fatty acids) in *Corallina pilulifera* tissue collected on December 22, 2012.

Fatty acids	Relative amount (%)
C14:0	1.9
C16:0	28.8
C18:0	6.3
C18:1 ω -9	1.7
C18:2 ω -6	3.8
C18:3 ω -6	1.5
C20:4 ω -6	5.3
C20:5 ω -3	31.4
C22:0	4.5
C22:2 ω -6	2.3
C24:0	1.5
Saturated fatty acids	50.7
PUFAs	45.4

Reference

- Agateuma Y, Mateuyama K, Nakata A, Kawai T, Nishikawa N. 1997. Marine algal succession on coralline flats after removal of sea urchins in Suttsu bay on the Japan Sea coast of Hokkaido, Japan. *Nippon Suisan Gakkaishi* 63: 672–680.
- Akioka H, Baba M, Masaki T, Johansen HW. 1999. Rocky shore turfs dominated by *Corallina* (Corallinales, Rhodophyta) in Northern Japan. *Phycological Research* 47: 199–206.
- AOAC. 2000. *Official Methods of Analysis*. Vol II, 17th ed. Association of Official Analytical Chemists. Washington, D.C.
- Baba M, Johansen HW, Masaki T. 1988. The segregation of three species of *Corallina* (Corallinales, Rhodophyta) based on morphology and seasonality in northern Japan. *Botanica Marina* 31: 15–22.
- Bailey JC and Chapman RL. 1998. A phylogenetic study of the Corallinales (Rhodophyta) based on nuclear small-subunit rRNA gene sequences. *Journal of Phycology* 34: 692–705.
- Bird CJ, Rice EL, Murphy CA and Ragan MA. 1992. Phylogenetic relationships in the Gracilariales (Rhodophyta) as determined by 18S rDNA sequences. *Phycologia* 31: 510 - 522.
- Bittner L, Payri CE, Maneveldt GW, Couloux A, Cruaud C, de Riviers B, Le Gall L. 2011. Evolutionary history of the Corallinales

(Corallinophycidae, Rhodophyta) inferred from nuclear, plastidial and mitochondrial genomes. *Molecular Phylogenetics and Evolution* 61: 697–713.

Clark G. 1981. *Staining Procedures*. 4th ed. Williams & Wilkins, Baltimore.

Freshwater DW, Fredericq S, Butler BS, Hommersand MH, Chase MW. 1994. A gene phylogeny of the red algae (Rhodophyta) based on plastid *rbcL*. *Proceedings of the National Academy of Sciences of the United States of America* 91: 7281–7285.

Guiry M.D. and Guiry G.M. 2012. AlgaeBase. <<http://www.algaebase.org>>(accessed May 2, 2012).

Hong YK, Kim SD, Polne-Fuller M, Gibor A. 1995. DNA extraction conditions from *Porphyra perforata* using LiCl. *Journal of Applied Phycology* 7: 103–107.

Itoh N, Izumi Y, Yamada H. 1985. Purification of bromoperoxidase from *Corallina pilulifera*. *Biochemical and Biophysical Research Communication* 131: 428–435.

Johnson CR, Mann KH. 1986. The crustose coralline alga, *Phymatolithon* Foslie, inhibits the overgrowth of seaweeds without relying on herbivores. *Journal of Experimental Marine Biology and Ecology* 96: 127–146.

Kim JH, Guiry MD, Oak JH, Choi DS, Kang SH, Chung H, Choi HG. 2007. Phylogenetic relationships within the tribe Janieae (Corallinales, Rhodophyta) based on molecular and morphological

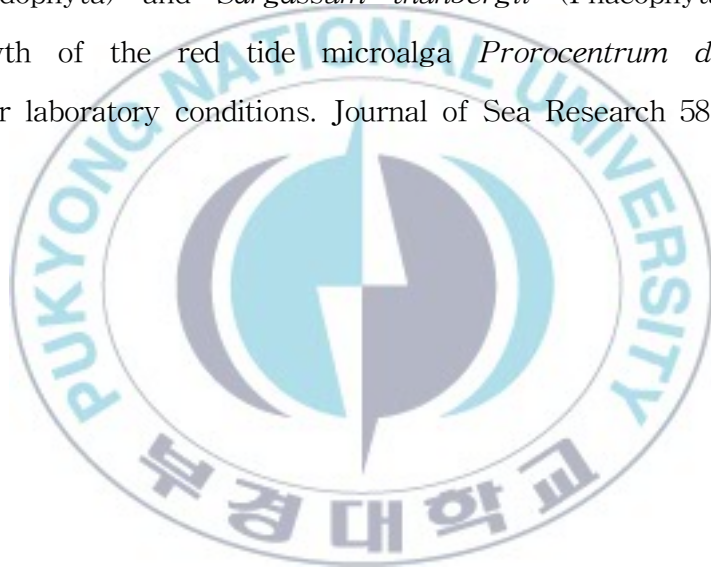
- data: a reappraisal of *Jania*. *Journal of Phycology* 43: 1310–1319.
- Kim MJ, Choi JS, Kang SE, Cho JY, Jin HJ, Chun BS, Hong YK. 2004. Multiple allelopathic activity of the crustose coralline alga *Lithophyllum yessoense* against settlement and germination of seaweed spores. *Journal of Applied Phycology* 16: 175–179.
- Kim MS, Yang EC, Boo SM. 2006. Taxonomy and phylogeny of flattened species of *Gracilaria* (Gracilariceae, Rhodophyta) from Korea based on morphology and protein-coding plastid *rbcL* and *psbA* sequence. *Phycologia* 45: 520–528.
- Kitamura H, Kitahara S, Koh HB. 1993. The induction of larval settlement and metamorphosis of two sea urchins, *Pseudocentrotus depressus* and *Anthocidaris crassispina*, by free fatty acids extracted from the coralline red algae *Corallina pilulifera*. *Marine Biology* 115: 387 - 392.
- Kumar S, Tamura K, Nei M. 2004. MEGA3: Integrated software for molecular evolutionary genetic analysis and sequence alignment. *Briefings in Bioinformatics* 5: 150–163.
- Kwon HJ, Bae SY, Kim KH, Han CH, Cho SH, Nam SW, Choi YH, Kim BW. 2007. Induction of apoptosis in HeLa cells by ethanolic extract of *Corallina pilulifera*. *Food Chemistry* 104: 196–201.
- Luyen QH, Cho JY, Choi JS, Kang JY, Park NG, Hong YK. 2009. Isolation of algal spore lytic C17 fatty acid from the crustose coralline seaweed *Lithophyllum yessoense*. *Journal of Applied Phycology* 21: 423–427.

- Masaki T, Fujita D, Hagen NT. 1984. The surface ultrastructure and epithallium shedding of crustose coralline algae in an Isoyake area of southwestern Hokkaido, Japan. *Hydrobiologia* 116/117: 218-223.
- Ohsawa N, Ogata Y, Okada N, Itoh N. 2001. Physiological function of bromoperoxidase in the red marine alga, *Corallina pilulifera*: production of bromoform as an allelochemical and the simultaneous elimination of hydrogen peroxide. *Phytochemistry* 58: 683-692.
- Park SM, Kang SE, Choi JS, Cho JY, Yoon SJ, Ahn DH, Hong YK. 2006. Viability assay of coralline algae using triphenyltetrazolium chloride. *Fisheries Sciences* 72: 912-914.
- Ryu BM, Qian ZJ, Kim MM, Nam KW, Kim SK. 2009. Anti-photoaging activity and inhibition of matrix metalloproteinase (MMP) by marine red alga, *Corallina pilulifera* methanol extract. *Radiation Physics and Chemistry* 78: 98-105.
- Saito N, Nei M. 1987. The neighbor-joining method: a new method for reconstructing phylogenetic tree. *Molecular Biology and Evolution* 4: 406-425.
- Thomas DN. 2002. *Seaweeds*. Smithsonian Institution Press, Washington, D.C.
- Tokuda H, Kawashima S, Ohno M, Ogawa H. 1994. *Seaweeds of Japan*. Midori Shobo Co., Tokyo.
- Walker RH, Brodie J, Russell S, Irvine LM. 2009. Biodiversity of

coralline algae in the northeastern Atlantic including *Corallina caespitosa* sp. (Corallinoideae, Rhodophyta). *Journal of Phycology* 45: 287–297.

Yan X. 1999. Assessment of calcareous alga *C. pilulifera* as elemental provider. *Biomass & Bioenergy* 16: 357–360.

Wang R, Xiao H, Wang Y, Zhou W, Tang X. 2007. Effects of three macroalgae, *Ulva linza* (Chlorophyta), *Corallina pilulifera* (Rhodophyta) and *Sargassum thunbergii* (Phaeophyta) on the growth of the red tide microalga *Prorocentrum donghaiense* under laboratory conditions. *Journal of Sea Research* 58: 189–197.



Chapter IV

Effect of calcification inhibitors on the viability of the coralline algae

Abstract

The addition of calcification inhibitors was found to regulate the viability of cultures of the coralline alga *Lithophyllum yessoense* and *Corallina pilulifera*. The viability was quantitated using a triphenyltetrazolium chloride assay, and the eight of different calcification inhibitors were tested. Fe-citrate and FeCl₂ inhibited viability, and dichloromethylenediphosphonic acid increased viability. The Fe-citrate, which had the strongest inhibitory activity, decreased viability to 74 and 12% that of the control following addition of 1 mM or 10 mM of culture media of *L. yessoense*, respectively. Even *C. pilulifera* culture media, Fe-citrate inhibited viability to 63 and 44% that of the control following addition of 1 mM or 10 mM. The Fe-citrate suppressed *L. yessoense* and *C. pilulifera* viability the most.

Key words: Crustose alga, Calcification, *Lithophyllum*, *Corallina pilulifera*, Anti-fouling

Introduction

Many areas of the rocky shorelines of Korea and Japan are currently dominated by crustose coralline algae such as *Lithophyllum yessoense* Foslie (Suzuki et al. 1998; Kim 2000). These non-articulated (non-geniculate) calcareous algae cover the surfaces of rocks in a pink or white-colored crust. The decrease in the seaweed flora of some rocky areas, known as alga whitening or barren ground, is associated with some species of crustose algae (Tokuda et al. 1994). Since 1990, the algal whitening area has expanded from south Cheju Island to the middle East Sea (Chung et al. 1998). In these areas, most fleshy seaweed has disappeared from rocks because of algal whitening, diminishing and devastating the food sources and spawning places of fish and shellfish. Algal whitening is now recognized as a natural hazard that adversely affects marine ecosystems and damages commercial fisheries (Kim 2002). When coralline algae are growing, the rock surfaces appear pink, while the fleshy seaweed flora disappears from the rocky areas. In marine environments, this phenomenon is generally called algal whitening, barren ground (Tokuda et al. 1994), coralline flats, or deforested areas. It is now recognized as a natural hazard adversely affecting marine ecosystems and damaging commercial fishing areas. Although biological (Kitamura et al. 1993; Agateuma et al. 1997) and physical (Masaki et al. 1984; Johnson and Mann 1986) factors may be sufficient to prevent the recruitment of fleshy seaweeds, allelopathic bromoform (Ohsawa et al. 2001) and fatty

acid (Kim et al. 2004; Luyen et al. 2009) substances may also inhibit the settlement or germination of seaweed spores. Consequently, coralline algae may also prevent fouling by fleshy seaweeds. Alternatively, biomimetic coralline alga material might become an environmentally friendly antifouling material. Biomimetic materials derived from the crustose coralline algae, containing antifouling substances, might be developed to protect against the attachment of soft foulants, especially micro- and macroalgae.

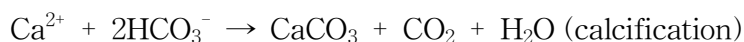
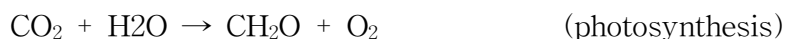
Calcium and inorganic carbon are the two major substrates of photosynthesis and calcification. Calcium chemistry is relatively simple because there is only one primary ionic species of this element, although various neutral and charged complexes of the divalent ion are known to exist in seawater (Kennish, 1994). In contrast, carbonate chemistry is much more complex because it involves a gaseous form and both ionic and neutral species as well as complexed forms in seawater (Gattuso et al. 1999).

Dissolved inorganic carbon (DIC) comprises 3 species: dissolved CO₂ (CO₂ + H₂CO₃) as well as bicarbonate (HCO₃⁻) and carbonate ions (CO₃²⁻)



Dissolved inorganic carbon is used by the animal host to deposit skeletal CaCO₃ and by the endosymbiont for its photosynthesis. Photosynthesis, respiration (of the animal and algal components) and

calcification can take place simultaneously according to the following simplified equations:



Photosynthesis and calcification both consume inorganic carbon but the combined processes can also be viewed as mutually supporting because CO_2 generated by calcification can be used for photosynthetic carbon fixation.

Biological mineralization is a complex phenomenon whereby calcium phosphate salts are transformed to hydroxyapatite, a process that may be influenced by natural inhibitors in the microenvironment. Certain chelating reagents are used to prevent the precipitation of minerals and are the active constituents in anti-scaling reagents and certain industrial cleaners, corrosion inhibitors and household detergents (Nancollas & Sawada, 1982; Fischer, 1993). For determining inhibition of coralline algae, we have used calcification inhibitors. The tissue viability of the coralline algae were quantitatively measured using a triphenyltetrazolium chloride assay.

Materials and Methods

Preparation of tissue

Coralline algae were collected from the rocky intertidal area at Cheongsapo (35°09'28" N, 129°11'47" E), on the east coast of Busan, Korea. The samples were transported in a container with seawater to the laboratory. After rinsing well with autoclaved seawater to remove epiphytes and debris, the encrusted tissues were sonicated three times with 30-spulses of an ultrasonic water bath (low-intensity frequency of 90kHz) to remove other microepiphytes. Non-articulated coralline tissue was then scraped off the stones using the saw. The tissue was thoroughly washed at least six times by centrifugation at $1000 \times g$ for 30 sec (Kang et al. 2005). Articulated coralline tissues were cleaned by brushing thoroughly and sonicating (47 kHz) twice for 1 min in autoclaved seawater, and immersed in 1% Betadine for 2 min to eliminate epiphytes (Jin et al. 1997). They were then rehabilitated at 18 °C in PES (Provasoli 1968) for a day before use.

Inhibitors

For calcification inhibitory agents, alendronate sodium trihydrate, dichloromethylenediphosphonic acid, etidronic acid, Fe-citrate, FeCl_3 , AlCl_3 , an inhibitor of hydroxyapatite, was dissolved on distilled water and added to a concentration of 10 mM and 1 mM, respectively. The

bicarbonate channel blocker, 4,4'-diisothiocyanatostilbene-2,2'-disulfonic acid was prepared the same way. The impermeable carbonic anhydrase inhibitor, acetazolamide was dissolved in dimethylsulfoxide.

Experimental set-up

To measure the viability of the tissue, 25 μL of each inhibitor was added to 5-mL PES medium containing 0.1 g of *L. yessoense* and 0.05 g of *C. pilulifera*, and the mix was cultured for 5 d at 16 °C with rotation at 130 rpm, under a photon flux density (fluorescent light) of 40 $\mu\text{mol m}^{-2}\text{sec}^{-1}$, and on a light cycle of 16-h light/8-h dark. A reference culture was prepared by mixing 25 μL distilled water or DMSO in the same medium. After harvesting the tissues by centrifugation at 3000 $\times g$ for 30 sec, the viability was measured using the TTC assay. The relative viability (%) was calculated as: $(S/C) \times 100$, where S equals the absorbance of tissue with seaweed extract and C equals the absorbance of the reference culture.

Viability assay

To measure the viability of the coralline tissue, the assay of Park et al. (2006) was used. Briefly, 1 ml of 0.8% 2,3,5-triphenyltetrazolium chloride (TTC) in seawater containing 50 mM Tris-HCl buffer (pH 8.0) was added to the tissue in a 1.7-ml microtube and incubated in darkness for 1.5 hr at 20 °C under mineral oil. The triphenyl formazan

that formed in the tissue was extracted with 0.6 ml of 0.2 N NaOH in 75% ethanol by heating for 15 min at 60 °C. The triphenyl formazan was quantified by measuring the absorbance at 475 nm.

Results

The effects of the calcification inhibitors on the viability of *Lithophyllum yessoense* were determined using the TTC assay after 5 d of culture. A reference culture lacking calcification inhibitors reached an absorbance of 1.27 ± 0.26 . To estimate the effects of the inhibitors on the viability of the coralline alga, we were determined 8 of calcification inhibitor samples. The inhibitors were added to *L. yessoense* culture medium to each concentration. Fe-citrate and FeCl_2 inhibited viability to 12 and 53% that of the control, respectively, whereas the dichloromethylenediphosphonic acid was show the viability to 100% at 10 mM (Table 4-1). At 1 mM, Fe-citrate inhibited viability to 74% that of the reference culture.

The effects of the calcification inhibitors on the viability of *Corallina pilulifera* were determined using the TTC assay after 5 d of culture. A reference culture lacking calcification inhibitors reached an absorbance of 1.10 ± 0.17 . Among determined calcification inhibitor samples, Fe-citrate and FeCl_3 inhibited viability to 44 and 35% that of the control, respectively at 10 mM (Table 4-2). At 1 mM, 4,4'

-diisothiocyanatostilbene-2,2' -disulfonic acid, Fe-citrate and ethidronic acid inhibited viability to 63%, 67% and 68% that of the control, respectively. The Fe-citrate suppressed *L. yessoense* and *C. pilulifera* viability the most. The Fe-citrate concentrations producing IC₅₀ were 3.5 mM, 3.8 mM for *L. yessoense* and *C. pilulifera*, respectively (Figure 4-1, 4-2).

Discussion

In reef-building corals, photosynthesis by endosymbiotic algae enhances calcification; this rate of calcification is reduced by shading and by inhibitors of photosynthesis such as DCMU (dichlorophenyl dimethyl urea) and Diamox and by some uncouplers of oxidative phosphorylation (Kawaguti & Sakumoto, 1948; Goreau, 1959; Goreau & Goreau, 1959; Yamazato, 1966; Yamashiro, 1995). These works show that the light-enhanced calcification can be reduced by inhibition of metabolic processes as a reduced supply of oxygen and organic materials which could enhance the calcification of the host coral. Calcification can also be reduced by compounds which prevent mineral deposition rather than affecting the metabolic processes. Also, Pentecost (1978) showed that calcification in the coralline alga *Corallina officinalis* is directly related to the photosynthetic rate, and Smith and Roth (1979) showed that the calcification rate is related to the inorganic carbon concentration in the medium.

Bisphosphonates, a group of synthetic chelating reagents containing a P-C-P bond, retard both formation (Francis et al. 1969) and dissolution (Fleisch et al., 1969) of calcium phosphates in vivo and in vitro. Bisphosphonates have been used in studies of calcification in calcareous algae (Okazaki et al. 1993) and mammals (Shinoda et al. 1983; Ohya et al. 1991) where they strongly inhibited mineral deposition. According to Yamashiro (1995), treatment by 1-hydroxyethylidene-1,1-bisphosphonic acid is able to block only calcification without a reduction of photosynthetically produced oxygen and organic materials supplied by the symbiotic algae.

Phosphocitrate and its analogue N-sulpho-2-amino tricarballylate were compared with ethane-1-hydroxy-1,1-diphosphonate for inhibition of calcium phosphate crystallization in hydroxyapatite induced crystal growth and ^{45}Ca uptake by matrix vesicles. Phosphocitrate (1 μM) was the most potent inhibitor followed by ethane-1-hydroxy-1,1-diphosphonate and N-sulpho-2-amino tricarballylate, the latter requiring a high concentration (100 μM) to be equally effective as an inhibitor (Shankar et al. 1983).

According to Suzuki et al. (1995), a medium enriched with iron promotes the growth of *Laminaria* and *Undaria*. In contrast, *Lithophyllum* grew even in an iron-limited medium ($< 1 \text{ nM Fe}$). In this study

Table 4-1. Effect of calcification inhibitors on viability of the coralline *Lithophyllum yessoense*¹.

Calcification Inhibitor	10 mM		1 mM	
	Absorbance at 475nm	Relative viability (%)	Absorbance at 475nm	Relative viability (%)
<i>Hydroxyapatite inhibitor</i>				
Alendronate	0.86±0.18	70	1.58±0.10	129
AlCl ₃	0.83±0.18	70	1.33±0.15	108
Dichloromethylene diphosphonic acid	1.27±0.35	103	1.50±0.06	122
Etidronic acid	0.91±0.42	74	1.22±0.29	100
Fe-citrate	0.15±0.06	12	0.94±0.44	76
FeCl ₃	0.67±0.15	55	1.14±0.38	93
<i>Bicarbonate channel blocker</i>				
4,4'-Diisothiocyanatostilbene-2,2'-disulfonic acid	ND	ND	1.71±0.31	139
<i>Carbonic anhydrase inhibitor</i>				
Acetazolamide	0.89±0.40	72	1.18±0.19	96

¹Reference culture without any calcification inhibitor reached absorbance of 1.27±0.26. Data are the mean ± SD (n≥3). ND; not determined.

Table 4-2. Effect of calcification inhibitors on viability of the coralline *Corallina pilulifera*¹.

Calcification Inhibitor	10 mM		1 mM	
	Absorbance at 475nm	Relative viability (%)	Absorbance at 475nm	Relative viability (%)
<i>Hydroxyapatite inhibitor</i>				
Alendronate	-	-	-	-
AlCl ₃	0.22±0.10	18	1.03±0.29	84
Dichloromethylene diphosphonic acid	0.90±0.24	73	0.81±0.23	66
Etidronic acid	0.64±0.28	54	0.66±0.24	54
Fe-citrate	0.50±0.25	40	0.65±0.22	53
FeCl ₃	0.39±0.21	31	1.18±0.19	96
<i>Bicarbonate channel blocker</i>				
4,4'-Diisothiocyanatostilbene-2,2'-disulfonic acid	ND	ND	0.61±0.19	50
<i>Carbonic anhydrase inhibitor</i>				
Acetazolamide	0.56±0.17	46	0.93±0.23	76

¹Reference culture without any calcification inhibitor reached absorbance of 1.11±0.15. Data are the mean ± SD (n≥3). ND; not determined.

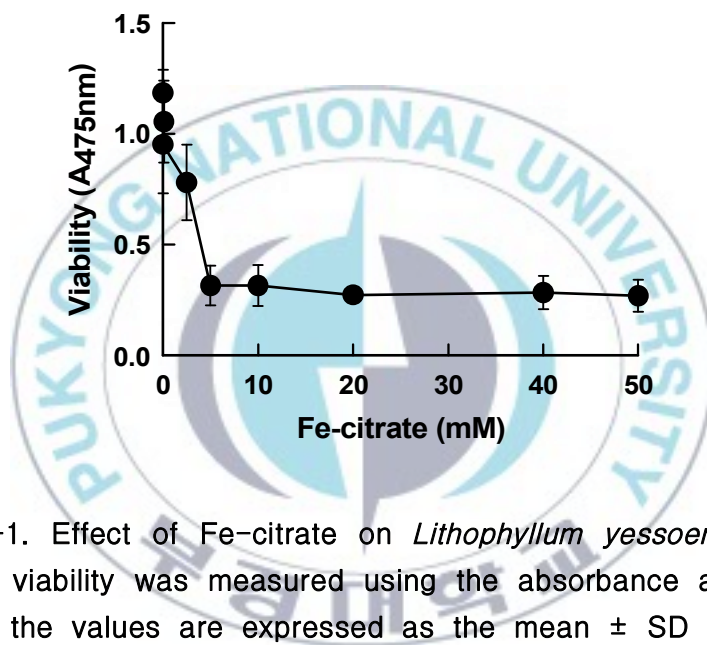


Figure 4-1. Effect of Fe-citrate on *Lithophyllum yessoense* tissue. The viability was measured using the absorbance at 475 nm, and the values are expressed as the mean \pm SD of at least five independent assays.

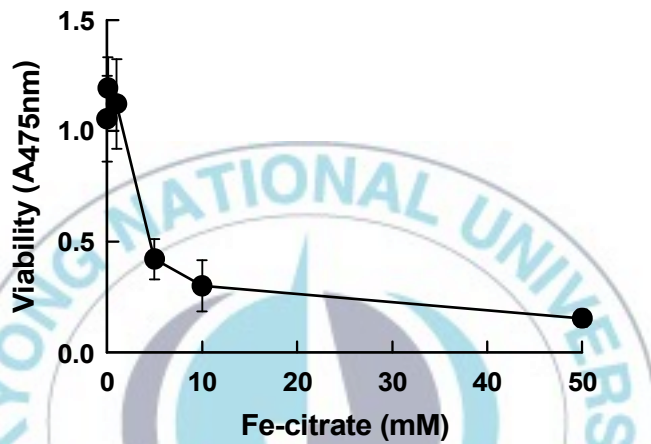


Figure 4-2. Effect of Fe-citrate on *Corallina pilulifera* tissue. The viability was measured using the absorbance at 475 nm, and the values are expressed as the mean \pm SD of at least five independent assays.

Reference

- Chung HS, Cho KW, Chung KH, Kim JH, Shin JH, Seo YW, Kang JS, Lee IK. 1998. Ecological characteristics of algal whitening in coastal zone of Seogwipo area, Cheju Island. *Algae* 13: 362-374.
- Gattuso JP, Allemand D, Frankignoulle M. 1999. Photosynthesis and Calcification at Cellular, Organismal and Community Levels in Coral Reefs: A Review on Interactions and Control by Carbonate Chemistry. *American Zoologist* 39: 160-183.
- Goreau TF. 1959. The physiology of skeleton formation in corals.I. A method for measuring the rate of calcium deposition by corals under different conditions. *Biological Bulletin* 116: 59-75.
- Goreau TF, Goreau N. 1959. The physiology of skeleton formation in corals.II. Calcium deposition by hermatypic corals under various conditions in the reef. *Biological Bulletin* 117: 239-250.
- Kang SE, Park SM, Choi JS, Ahn DH, Kim YD, Hong YK. 2005. Effect of seaweed extracts on the crustose coralline *Lithophyllum yessoense*. *Journal of fisheries science and technology* 8(4): 244-246.
- Kawaguti S, Sakumoto D. 1948. The effect of light on the calcium deposition of corals. *Bull. Oceanogr. Inst. Taiwan*, 4: 65-70.
- Kim JH. 2000. Taxonomy of the Corallinales, Rhodophyta, in Korea. Dissertation, Seoul National University, Korea.
- Kim HG. 2002. Ecological studies of seaweed in artificial seaweed bed.

In: Construction of Artificial Seaweed Bed for the Production Improvement in East Coast. East Sea Fisheries Research Institute, Korea. 31-41.

Kim MJ, Choi JS, Kang SE, Cho JY, Jin HJ, Chun BS, Hong YK. 2004. Multiple allelopathic activity of the crustose coralline alga *Lithophyllum yessoense* against settlement and germination of seaweed spores. *Journal of Applied Phycology* 16:175-179.

Luyen QH, Cho JY, Choi JS, Kang JY, Park NG, Hong YK. 2009. Isolation of algal spore lytic C17 fatty acid from the crustose coralline seaweed *Lithophyllum yessoense*. *Journal of Applied Phycology* 21: 423-427.

Park SM, Kang SE, Choi JS, Cho JY, Yoon SJ, Ahn DH, Hong YK. 2006. Viability assay of coralline algae using triphenyltetrazolium chloride. *Fisheries Sciences* 72: 912-914.

Provasoli L. 1968. Media and prospects for the cultivation of marine algae. In Watanabe A, Hattori A (eds), *Cultures and Collection of Algae*. The Japanese Society of Plant Physiologists, Tokyo, pp. 63 - 75.

Shankar R, Brown MR, Wong LK, Sallis JD. 1984. Effectiveness of phosphocitrate and N-sulpho-2-amino tricarballylate, a new analogue of phosphocitrate, in blocking hydroxyapatite induced crystal growth and calcium accumulation by matrix vesicles. *Experientia* 40: 265-267.

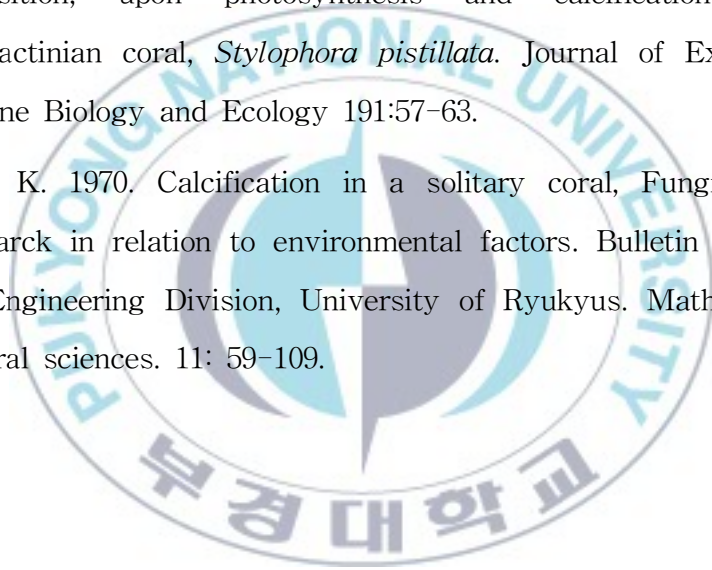
Suzuki Y, Takabayashi T, Kawaguchi T, Matsunaga K. 1998. Isolation

of an allelopathic substance from the crustose coralline algae, *Lithophyllum* spp., and its effect of on the brown alga, *Laminaria religiosa* Miyabe (Phaeophyta). *Journal of Experimental Marine Biology and Ecology* 225: 66 - 77.

Tokuda H, Kawashima S, Ohno M, Ogawa H. 1994. *Seaweeds of Japan*. Midori Shobo Co, Tokyo.

Yamashiro H. 1995. The effects of HEBP, an inhibitor of mineral deposition, upon photosynthesis and calcification in the scleractinian coral, *Stylophora pistillata*. *Journal of Experimental Marine Biology and Ecology* 191:57-63.

Yamazato K. 1970. Calcification in a solitary coral, *Fungia scutaria* Lamarck in relation to environmental factors. *Bulletin of Science & Engineering Division, University of Ryukyus. Mathematics & natural sciences.* 11: 59-109.



Chapter V

Antifouling activity of extracts of the periostracum of the mussel *Mytilus edulis*

Abstract

A study was made to investigate possible formation by the periostracum of the mussel *Mytilus edulis* of antifouling substances against the settlement and germination of spores of *Porphyra suborbiculata*. The shell coating known as the periostracum, is indicated as a possible physical and chemical antifouling defense component. The periostracum was separated from the shell and extracts of the periostracum obtained by extraction with three solvents. Considerable activity against monospores was shown by ethyl acetate and dichloromethane extract. The microtopography of the shell surface was measured using scanning electron microscopy (SEM) which revealed homogeneous and ridged surface of periostracum. The periostracum surface has also shown considerable activity against monospores. This indicates that in mussels *P. suborbiculata* the periostracum possesses a generic anti-settlement property, at least against spores settlement and germination.

Key words: antifouling, periostracum, *Mytilus edulis*, *Porphyra suborbiculata*

Introduction

Biofouling is a natural process of marine ecosystem caused by the surface colonization and development of micro and macrofoulers on submerged natural/man-made marine structures, leading to huge economic and environmental losses worldwide. The annual global loss of maritime domain is more than 6.5 million dollars (Bhadury et al. 2004). Fouling of ship hulls and niche areas represents a significant cost for the maritime industry. Higher maintenance costs, increased fuel requirements due to greater levels of hull drag, lost productivity due to more frequent dry-docking for removal of fouling organisms, and the cost of compliance with environmental regulations create a significant burden for maritime operators, whether private or public (Callow et al. 2003; Statz et al. 2006; Yebra et al., 2004). Previously utilized antifouling agents, such as widely used vessel biocidal coatings containing the organotin ‘Tributyltin’ (TBT), although efficacious against fouling, have limitations relating to their toxicity (Anderson et al. 2003; Statz et al. 2006). The toxicity of TBT in the marine environment has been extensively researched, with evidence of oyster deformities, imposex in dog whelks, adverse effects on marine benthic organisms and concentration and accumulation in the marine food chain (Callow et al. 2002; Sonak 2008). As a result of these environmental impacts, TBT is the subject of a relatively recent worldwide ban by the International Maritime Organisation (IMO). As of January 2008, vessels of countries party to the convention and those

engaged in activities at ports of convention parties, are no longer permitted to have TBT containing coatings on vessels of any size (IMO 2001). Due to these limitations with conventional coatings, research into 'biomimetics'-surfaces and compounds inspired by natural systems - capable of resisting fouling pressure whilst reducing impacts on the local and extended environments has grown importance (Scardino et al. 2009; Rolston et al. 2009; Scardino et al. 2011). It has been observed that some marine species such as mussels are able to resist fouling when in good physiological condition (Abarzua et al. 1995; Wahl 1998; Scardino et al. 2003; Scardino et al. 2004; Bers et al. 2006a). Mussels have a tough, yet pliable, proteinaceous shell covering secreted by the mantle, which is known as the 'periostracum' (Harper et al. 1993, Scardino et al. 2003). Scardino et al. (2003) and Bers et al. (2006b) noted that fouling organisms showed some preference toward compromised areas of the periostracum for initial attachment and that mussels with an intact periostracum showed a greater resistance to fouling pressure. Several studies have recorded the influence of a physical fouling deterrent in the form of microtopography on mussel shells (Wahl et al. 1998; Bers et al. 2004; Scardino et al. 2004). Bers et al. (2006b) suggested that in conjunction with the recognized physical antifouling defenses of marine mussels (such as 'weeping' of the shell by the foot), there appears also to be a chemical element to the defence. Bers et al. (2006b) were able to demonstrate some antifouling activity toward a variety of common fouling organisms from the extracts take from the periostracum of the marine blue

mussels, *Mytilus edulis* without separating periostracum from the rest of the mussel shell.

The aim of this study was to investigate antifouling activity of periostracum extracts of *M. edulis*. When separated from the shell, against alga *Porphyra suborbiculata* monospores settlement and germination and to attempt to isolate and identify extracts responsible for the antifouling inhibition.

Materials and Methods

Monospore culture

Juvenile blades of *Porphyra suborbiculata* were collected from the rocky intertidal area at Cheongsapo (35°09'28" N, 129°11'47" E), on the east coast of Busan, Korea. The fresh blades were rinsed, sonicated (low-intensity frequency of 90 kHz) twice for 1 min in autoclaved seawater, and immersed in 1% Betadine solution with 2% Triton X-100 for 1 min to eliminate epiphyte. To liberate the monospores, blades were cultured in Provasoli enriched seawater (PES) medium (Provasoli 1968) under 40 $\mu\text{mol m}^{-2}\text{s}^{-1}$ light intensity (10L:14D) at 20 °C. Monospores were then grown to juvenile blades under the same conditions.

Mussel shells

Mussel shells (62.5 ± 3.3 mm length) were collected from Namcheon fish market. Shells which were covered by fouling or damage were discarded. Shells with obvious existing fouling, severely damaged shells or noticeably abraded periostracum were also rejected. Specimens were gently cleaned of associated detritus (mud, debris, byssal threads etc) and any obvious microfouling films, prior to submersion in the vinegar solution.

Periostracum extract

Whole shells were submerged in a vinegar and seawater 'pickling' solution to aid removal of the periostracum. A 1:2 vinegar: seawater mixture (approximately 2% acetic acid), was found to be most effective to loosen the periostracum. Samples were retained in the pickling solution for approximately 24 hours, after which time the periostracum was peeled from the shell with forceps and stored in seawater. The periostracum peels were washed with distilled water to remove excess associated salts and acetic acid and then one part of peels were frozen to -20 °C prior to freeze-dry and, other peels to be use for fouling test and spores culture.

Freeze dried periostracum were ground to a powder for 5 min using hand mortar. 20 mg of periostracum powder was each extracted with 1 mL of one of the following slovents: dichloromethane (DCM),

ethyl acetate (EA), methanol (MeOH) and dimethyl sulfoxide (DMSO). Extraction with each solvent was repeated three times for 1 h by pulses of an ultrasonic water bath (low-intensity frequency of 90 kHz) and the combined extracts were dried under nitrogen. A stock solution of each extraction was prepared by the addition of 1 mL dimethyl sulfoxide (DMSO) to each 40 mg of dried extract. The prepared stocks were filtered through a 0.45 μm syringe filter before use.

Spores bioassay

For assay of spore settlement, aliquots of 100 μL seawater were at first distributed in a 96-well plate. 1 μL of seaweed extract (40 mg mL^{-1}), 4 μL PES stock and approximately 100 - 200 spores were added, and the final volume made immediately to 200 μL . For algal conditioned seawater, approximately 100 - 200 spores were centrifuged and 200 μL aliquot of the conditioned water was added. The resulting spore suspensions were placed in the dark for 1 day at 18 $^{\circ}\text{C}$ to allow for even settlement on the bottom. At the end of this period, non-settled spores were removed from the bottom by centrifugation in an inverted position at $1500 \times g$ for 15 min. The number of settled spores was counted under a microscope after replacing with new PES solution. Spore settlement was expressed as the percentage of the reference value. The reference material for each test was prepared using the same procedure apart from the absence of extract. The minimum detectable inhibition of spore settlement by DMSO occurred

at 0.5% (data not shown). Therefore the final concentration of DMSO was kept below 0.5% in all tests.

For assay of spore germination, approximately 100 - 200 spores were added to a 200 μL aliquot of PES in a 96-well plate, and placed in the dark for 1 day at 18°C to settle spores on the bottom. After non-settled spores were removed from the bottom by centrifugation in an inverted position, and fresh 200 μL PES was added, then 1 μL of each extract (40 mg mL^{-1}) was immediately added to each 200 μL culture. The resulting germling cultures were placed at 18 °C and 80 $\mu\text{mol m}^{-2}\text{s}^{-1}$ light intensity on a 12L:12D cycle for 1 wk to permit development. The number of germling was counted under the microscope and expressed as a percentage of the reference culture. The minimum DMSO concentration leading to detectable inhibition was 0.5% (data not shown). Therefore the solvent extracts and reference solutions were always added to the medium to provide a DMSO concentration in the assay cultures <0.5%. The experiments were repeated at least three times with each independent

Results

Approximately 200 monospores of *Porphyra suborbiculata* were allowed to a 96-well plate, while spores could not settled well at periostracum of *Mytilus edulis* (Fig. 5-1). The periostracum of *M.*

edulis showed significant germination inhibition (86%) compared to the reference.

M. edulis had a microtopography with a regular corrugated ridging pattern under SEM (Figure 5-1). The periostracum of *M. edulis* is covered by microripples, 1 - 1.5 μm wide, running parallel to each other and orthogonal to the growth rings of the mussel shell. They stretched across the entire shell, without branching or broadening in any area of the shell.

Antifouling activities of the periostracum extracts of *Mytilus edulis* were examined on spore settlement and germling of the *Porphyra suborbiculata*. Dichloromethane (DCM), ethyl acetate (EA), methanol (MeOH)-soluble fraction were isolated from fresh and acidified periostracum to confirm the activity. When 200 $\mu\text{g mL}^{-1}$ of each extracts were added to spores in the settlement assay, DCM extract of the fresh periostracum showed settlement inhibition of 11% against the reference (Table 5-1). The study was continued by investigating possible effects on spore germination (Table 5-2). Against *P. suborbiculata*, the 200 $\mu\text{g mL}^{-1}$ DCM and EA extract of the acidified periostracum reduced monospore germination to 5 and 7% of control. The study was continued by investigating possible effects of periostracum its self on spore germination. When 200 $\mu\text{g mL}^{-1}$ DMSO extract were added to an acidified inner periostracum and outer periostracum, the germling rate was showed 14 and 12%, respectively. 10 compounds in the DCM extract identified by GC-MS (Table 5-3). Of the identified compounds, the major compound was oleamide (19%).

Discussion

This research has shown antifouling activity of extracts of marine mussel's periostracum against common fouling organisms. The results of this research have shown some antifouling activity in extracts of the periostracum obtained from the *Mytilus sp.* (Berset. 2006). The spores assay show that antifouling activity is greater in extracts produced from dichloromethane and ethyl acetate rather than methanol. This suggests that the compound responsible for activity is relatively non-polar. Significant difference was observed between extracts and control in the spores settlement and germination.

Statistical analysis of results was unable to be performed for the settlement and germination of spores on periostracum tissue for this study due to the number of factors. The high levels of autofluorescence demonstrated by periostracum tissue prevented accurate microscopic counting of the spores on images, and hence no accurate quantitative analysis of the settlement and germination inhibition of the periostracum could be made. The small data set from the spores assay meant that any statistical interpretation would not be robust. However it was shown that the periostracum had a deterrent effect on the settlement and germination of spores. Previous research into antifouling characteristics of marine mussel shells has shown that the microtopography of the shell may be a physical deterrent to barnacle cyprid settlement, and hence, chemical activity toward barnacle cyprinids may not be as pronounced (Scardino and Nys 2004).

On the study of fouling organism on the mussel shells, we observed that the shell of aquaculture mussels had intact periostracum while the periostracum of wild mussels was not intact. Thus the shells of aquaculture mussels were largely unfouled compare to the shell of wild mussels which were largely fouled by fouling organisms. The strong correlation between the presence of an intact periostracum and a low level of fouling is consistent with its role as an antifouling mechanism. Studies in which periostracum has been experimentally removed also indicate as role for this shell layer in antifouling. For example, fouling by algae and barnacles on *M. edulis* was significantly greater on areas of shell where the periostracum had been physically removed (Wahl et al. 1998). Preference for areas of the shell where the periostracum is abraded or absent, such as on older shell, has been observed for a diversity of molluscs fouled by a range of boring organisms including endolithic algae (Kaehler 1999), sponges and other invertebrates (e.g. Mao Che et al. 1996). The end result of these infestations is often death of the host (Mao Che et 1996; Kaehler and McQuaid 1999).

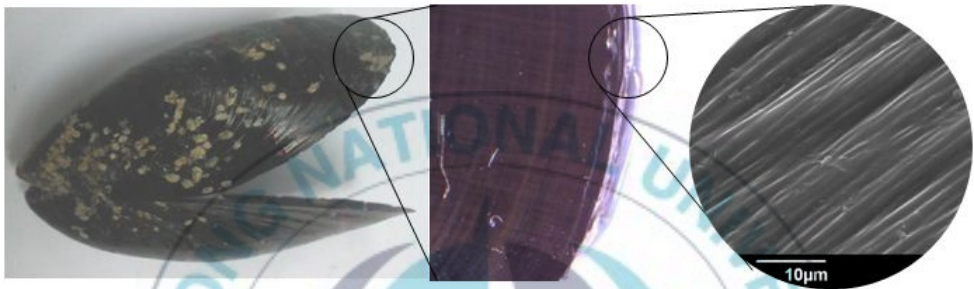


Figure 5-1. Periostracum of blue mussel *Mytilus edulis*.

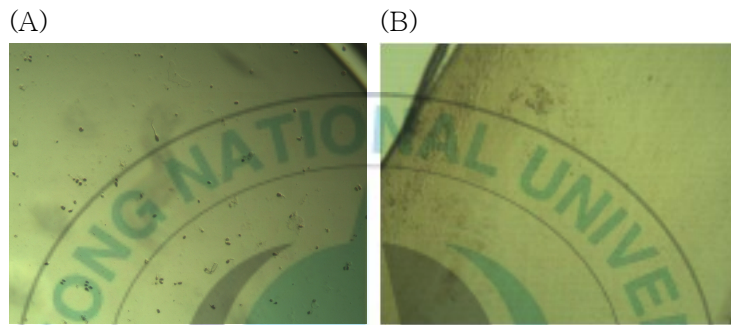


Figure 5-2. Settlement of *Porphyra suborbiculata* monospores on periostracum of *M. edulis*.

Table 5-1. Effects of extracts from periostracum on settlement of *Porphyra suborbiculata* monospores.

	Solvent	Settlement (400 $\mu\text{g mL}^{-1}$)
Acidify outer	DCM	35 \pm 17
	EA	41 \pm 7
	MeOH	55 \pm 9
Acidified inner	DCM	31 \pm 7
	EA	32 \pm 1
	MeOH	34 \pm 6
Fresh inner	DCM	35 \pm 5
	EA	37 \pm 9
	MeOH	47 \pm 8

Notes: Value are expressed as percentage of control. Data are mean \pm SD for at least 3 independent assays. Average percentage of settled spores in reference is 81.0 \pm 7.8%.

Table 5-2. Effects of extracts from periostracum on germination of *Porphyra suborbiculata* monospores.

	Solvent	Germination (400 $\mu\text{g mL}^{-1}$)
Acidify outer	DCM	5.1 \pm 1.8
	EA	8.9 \pm 2.4
	MeOH	10.6 \pm 5.0
Acidified inner	DCM	3.5 \pm 3.2
	EA	5.2 \pm 2.6
	MeOH	10.6 \pm 2.4
Fresh inner	DCM	3.4 \pm 5.4
	EA	4.5 \pm 4.1
	MeOH	16.5 \pm 3.6

Notes: Value are expressed as percentage of control. Data are mean \pm SD for at least 3 independent assays. Average percentage of germinated per settled spores in reference is 83.2 \pm 5.9%.

Table 5-3. Composunds identified from dichloromethane extracts of periostracum by GC-MS.

RT	compounds	relative peak area (%)
8.383	Nonanal	1.49
10.933	Pelargonic acid (C7:0)	0.32
17.683	Myristic acid (C14:0)	0.37
21.467	Palmitic acid (C16:0)	0.31
22.833	Phytol	0.28
23.567	STEARIC ACID (C18:0)	0.38
33.3	Oleamide	19.00
37.783	1-Tetracosanol	8.89
38.05	Cholest-5-en-3-ol	3.61
40.4	1-Pentacosanol	3.91
-	Unknowncompounds	61.44

Reference

- Agateuma Y, Mateuyama K, Nakata A, Kawai T, Nishikawa N. 1997. Marine algal succession on coralline flats after removal of sea urchins in Suttsu bay on the Japan Sea coast of Hokkaido, Japan. *Nippon Suisan Gakkaishi* 63: 672-680.
- Abarzua S, Jakubowski S. 1995. Biotechnological investigation for the prevention of biofouling. I. Biological and biochemical principles for the prevention of biofouling. *Marine Ecology Progress Service* 123: 302-312.
- Bears AV, Wahl M. 2004. The Influence of Natural Surface Microtopographies on Fouling. *Biofouling* 20: 43-51.
- Callow ME, Callow JA. 2002. Marine Fouling: A Sticky Problem, *Biologist* 49: 1-5.
- Callow ME, Callow JA. 2003. Some New Insights into Marine Fouling. *World super Yacht* 1: 35-39.
- Harper EM, Skelton PW. 1993. A Defensive Value of the Thickened Periostracum in the Mytiloidea. *The Veliger* 36: 36-42.
- Scardino A, de Nys R, Ison O, O'Connor W, Steinberg P. 2003. Microtopography and antifouling properties of the shell surface of the bivalve molluscs *Mytilis galloprovincialis* and *Pinctada imbricata*. *Biofouling* 19(Suppl.): 223-30.
- Scardino AJ, de Nys R. 2004. Fouling deterrence on the bivalve shell

Mytilus galloprovincialis: a physical phenomenon? Biofouling 20: 249-257.

Scardino A, de Nys R. 2011. Biomimetic Models and Bioinspired Surfaces for Fouling Control. Biofouling 27: 73-86.

Scardino AJ, Zhang H, Cookson DJ, Lamb RN, de Nys R. 2009. The role of nano-roughness in antifouling. Biofouling 25: 757 - 767.

Sonak S, 2009. Implications of organotins in the marine environment and their prohibition. Journal of Environmental Management 90(Suppl.): S1-S3.

Statz A, Finlay J, Dalsin J, Callow M, Callow JA, Messersmith PB. 2006. Algal antifouling and fouling-release properties of metal surfaces coated with a polymer inspired by marine mussels. Biofouling 22: 392-399.

Thiyagarajan V, Nair KVK, Subramoniam T, Venugopalan VP. 2002. Larval settlement behaviour of the barnacle *Balanus reticulatus* in the laboratory, Journal of the Marine Biological Association of the UK 82: 579-582.

방오소재 개발을 위한 산호조류 및 진주담치 각피의 생물학적 특성

강지영

부경대학교 일반대학원 생물공학과

요약

본 연구에서는 선박이나 해양구조물에 부착하는 오손생물에 의한 피해를 방지하기 위하여 부작용 없는 환경친화적인 생체모방형 방오소재의 개발을 위하여 산호조류와 담치의 각피로부터 방오소재를 탐색하고자 하였다.

연안 암반지역에서 해조류 군락의 소실 즉 백화 혹은 갯녹음현상은 산호조류와 관련성이 있다. 대표적인 무절산호조의 생물학적 특성을 파악하기 위하여 18S rDNA 유전자를 분석한 결과 흑돌잎 (Lithophyllum) 속에 속하는 것을 확인하였고 그 형태적 특성으로 보아 *L. yessoense* 종인 것으로 유추된다. Triphenyl tetrazolium chloride 로서 활력을 측정된 결과 12월에서 2월 사이가 가장 높았으며, 조직 활력을 유지하기 위하여는 16°C, 16:8 시간 광주기, 30 $\mu\text{E}/\text{m}^2/\text{s}$ 광도에서 5일간 최적상태를 보였다. 지방산 조성에서는 EPA 가 가장 많은 고도불포화지방산으로서 9.7%를 차지하고 있다. 주사형전자현미경에 의한 표면구조를 보면 평균 3.6 μm 직경의 둥근 함몰 분화구 모양을 이루며 그 위에 1.0 내지 3.7 μm 의 비정형 다각형 구조물들이 덮여져 있다.

또한 백화현상에 연관되는 무절산호조류가 서식하는 지역에서는 유절산호조류도 함께 서식하고 있다. 이에 유절산호조에 대한 방오소재로서의 가능성을 확인하기 위하여 대표적 유절산호조류 종인 작은구슬산호말에 대하여 연구를 수행하였다. 채집된 산호조류는 가지 끝부분의 가장자리가 흰색을 나타내며 일반적 식물체는 석회질 성분으로 작은구슬산호말의 형태학적 특성을 가지며, 절간 당 medullary tiers 수는 12 에서 16 사이였으며, 절간의 길이는 약 1.0 - 1.4 mm 로 나타났다. 18S rDNA, psbA, rbcL gene sequence 를 비교해본 결과, 작은구슬산호말 (*Corallina pilulifera*)로 동정되었다. 유절산호조류의 계절적 활력 Triphenyl tetrazolium chloride 로서 활력을 측정된 결과 12월에서 1월 사이가 가장 높았으며, 조직 활력을 유지하기 위하여는 16°C, 16:8 시간 광주기, 40 $\mu\text{E m}^{-2}\text{s}^{-1}$ 광도에서 3일간 최적상태를 보였다. 지방산 조성에서는 EPA 가 가장 많은 고도불포화지방산으로서 31.4%를 차지하고 있다. 주사형전자현미경에 의한 표면구조를 보면 평균 7.9 \pm 1.3 μm 직경의 둥근 구멍들로 덮혀져 있으며 이러한 well 모양의 구조 대부분은 수직 콘을 형성하며 불규칙적으로 이루어져있다.

산호조류의 생물학적 특성연구와 함께 산호조류의 2차적 오손을 방지하기 위하여 산호조류에 기존에 알려진 석회화 저해제 (calcification inhibitor)를 첨가하여 산호조류의 활성억제 내지는 사멸 물질을 탐색하였다. 납작돌잎 (*L. yessoense*)과 작은구슬산호말 (*C. pilulifera*)을 대상으로 calcification inhibitor 의 산호조류 활력에 대한 영향을 알아보기 위하여 무균처리한 시료를 PES 배지에서 16°C, 40 $\mu\text{E m}^{-2}\text{s}^{-1}$ 광도, 16:8 시간 광주기 하에 5일 동안 배양하였으며 대조군은 저해제를 제외한 증류수만 첨가하였다. 시료에 대하여 2,3,5-triphenyltetrazolium chloride 에 의하여 viability 를 측정하였으며 그 값은 파장 475 nm 에서 측정하여 사용하였으며, 대조군에 대한 relative inhibition 값으로 나타내었다. 8 종의 저해제 중 납작돌잎에 대하여 dichloro methylene

diphosphonic acid 가 10 mM 에서 100%를 보인 반면, Fe-citrate 는 10mM 과 1mM 에서 각각 12%, 53%의 활력을 나타내어 가장 높은 사멸활성을 보였다. 저해제를 처리하지 않은 작은구슬산호말 조직의 경우에는 475 nm 파장에서 1.10 ± 0.17 의 흡광도 값을 나타내었다. 처리된 저해제 중에서 $AlCl_3$ 가 10 mM 에서 대조군에 대하여 39%의 활력을 나타내어 높은 활성을 보였으나, 1 mM 에서 그 값이 매우 낮게 나타났다. Fe-citrate 와 $FeCl_3$ 는 10 mM 에서 대조군에 대하여 각각 44%, 35%를 보였다. 2 종의 산호조류에 대하여 저해능이 높게 나타낸 Fe-citrate 가 가장 석회화 저해제로서 적합하다고 사료되어졌으며, 작은구슬산호말에 대한 농도별 Fe-citrate 의 영향을 조사한 결과, IC_{50} 값은 3.8 mM 로 나타났다.

산호조류와 함께 생체모방형 소재 후보로서 진주담치 (*Mytilus edulis*)의 각피 (periostracum)의 해조류 포자에 대한 방오활성을 조사한 결과, 박피한 진주김치의 periostracum 에 중성포자의 부착과 발아가 저해됨을 확인하였다. 김 중성포자에 대하여 periostracum 의 유기용매 (methanol, ethyl acetate, dichloromethane) 추출물들은 대조군에 비하여 32 - 62%의 부착 저해율을 보였다. 또한 김 중성포자의 발아에 대해서도 80 - 96%의 저해율을 나타냈다. Periostracum 의 유기용매 추출물 중 dichloromethane 추출물이 중성포자의 부착과 발아에 대하여 대조군에 비하여 62%, 96% 로 가장 높은 저해율을 나타냈다. Periostracum 의 dichloromethane 추출물의 GC-MS 분석 결과, 지방산 유도체인 oleamide 가 19%로 가장 함유량을 보였다.

상기 연구결과를 통하여 산호조류와 담치 각피의 조성과 구조를 바탕으로 환경친화적 생체모방형 방오소재의 활용 및 방오소재의 2차적인 오손을 방지하기 위한 첨가제로서 활용 가능할 것으로 여겨진다.



Acknowledgements

논문을 준비하면서 많이 부족하고 힘이 들 때도 있었지만 많은 분들의 격려와 도움으로 졸업논문을 완성할 수 있었습니다. 길지만 부족함이 많았던 시간동안 학부, 석사, 박사과정을 지내며 많은 가르침을 주신 홍용기 교수님께 감사드리며 알찬 결과로 답하지 못하여 죄송한 마음입니다. 그동안 많은 관심과 조언을 주신 박남규 교수님과 김종균 교수님, 오랜 시간 가르침을 주신 이형호 교수님, 공인수 교수님, 김성구 교수님, 정귀택 교수님, 바쁘신 와중에도 논문 심사와 조언을 주신 황동수 교수님과 문일수 교수님께도 정말 감사드립니다.

매번 귀찮게 질문하고 부탁드려도 자상하게 도와주시고 조언과 격려를 주신 조지영 교수님, 진형주 교수님, 간간한 실험실 생활에도 잘 지내준 황선영, 이익준, 최지영 후배님, 그리고 많은 외국인 친구들, 생물공학과 학우들에게도 감사의 말을 전합니다.

I wish to express my cordial thanks to all of my friends, Prof. Mohammed Nurul Absar Khan, Dr. Mumammad Tanvir Hossain Chowdhury, Paulos Getachew, Maddy, Hashim, Siti, Ian, Dr. Md Abdul Hannan Dr. Luyen Qouc Hai, Thi Hoai Luguen, Dr. Bangoura Issa, Dr. Md Salim Uddin for their helpfulness, well understanding, and providing excellent working atmosphere to carry out my research work throughout the whole period.

늘 격려해 주신 서정길 박사님, 문호성 박사님, 안상중 박사님, 김동균 박사님, 은민언니, 윤임언니, 유미언니, 유정언니, 든든한 생공오투 수경, 현진, 주희, 남희, 미진, 혜연, 예쁜 후배 은정, 규유, 부경대에 있으면서 많은 도움을 주신 분들께 감사의 말을 전합니다. 그리고 언제나 격려와 용기를 주신 희영언니, 연지, 현경, 희진언니, 리아식구 선영, 정희, 병하에게 고마움을 전합니다.

지칠 때는 힘이 되어주고 어이없는 투정도 받아주며 언제나 곁에서 격려해주로 지켜봐준 문헌식군에게 진심을 다해 고마움을 표현합니다.

긴 시간동안 고맙게 기다려준 언니들과 형부들, 사랑스런 조카들, 이모와 이모부, 세상에 하나뿐인 동생 강보승군과 어머니께 감사와 사랑의 말을 전하며, 마지막으로 늘 보고 싶은 아버지께 사랑을 전합니다.